

## TUTORIAL REVIEW

[View Article Online](#)  
[View Journal](#)

Cite this: DOI: 10.1039/d5su00426h

**Bacterial cellulose: a sustainable nanostructured polymer for biosensor development**Mojdeh Mirshafiei,<sup>a</sup> Amir Keshavarz Afshar,<sup>b</sup> Fatemeh Yazdian,<sup>ID \*b</sup> Hamid Rashedi,<sup>\*a</sup> Abbas Rahdar<sup>ID c</sup> and M. Ali Aboudzadeh<sup>ID \*d</sup>

Biosensors represent a transformative class of analytical devices that convert the recognition of target analytes into quantifiable signals, offering enhanced accuracy, sustainability, and rapid response times through the selective detection of specific biomarkers. In response to growing demands for environmentally sustainable and high-performance technologies, the field is increasingly shifting toward renewable materials. Among these alternatives, bacterial cellulose (BC) has garnered significant attention as a promising sustainable platform for next-generation biosensors. This review provides a comprehensive overview of BC, encompassing its biosynthesis pathways, intrinsic physicochemical features, and versatile functionalization strategies for tailored biosensing performance. By focusing on the design and fabrication of BC-based biosensors, with an emphasis on coupling biorecognition elements to various transduction platforms, this review highlights their burgeoning applications across the domains of healthcare, environmental monitoring, and food safety. It then expands the discussion to their roles in early disease diagnosis, real-time wound monitoring, wearable health tracking, and point-of-care testing, as well as detection of pathogens, pesticides, and heavy metals. Further, the emerging role of artificial intelligence (AI) in enhancing biosensor data analysis is explored, and finally concludes by discussing current challenges and future perspectives.

Received 10th June 2025

Accepted 5th November 2025

DOI: 10.1039/d5su00426h

[rsc.li/rscsus](https://rsc.li/rscsus)**Sustainability spotlight**

This review highlights the sustainable advancement of biosensor technology through the use of bacterial cellulose (BC), a renewable, biodegradable, and biocompatible biopolymer. BC presents a viable alternative to conventional, non-renewable substrates such as plastics and glass, offering superior properties including high mechanical strength, purity, and tunable porosity. Its suitability for surface modification enables the development of highly sensitive, selective, and minimally invasive biosensors applicable in healthcare, environmental monitoring, and food safety. By emphasizing BC-based platforms, this review aligns with the UN Sustainable Development Goals, specifically SDG 3 (Good Health and Well-being), SDG 9 (Industry, Innovation, and Infrastructure), SDG 12 (Responsible Consumption and Production), and SDG 13 (Climate Action), and underscores the potential of sustainable materials in advancing next-generation sensing technologies.

**1. Introduction**

The term “biosensor” refers to a compact analytical device that integrates a biological recognition element with a physicochemical transducer to produce a quantifiable signal upon interaction with a target analyte.<sup>1</sup> This enables rapid, real-time,

accurate, and specific detection, rendering biosensors invaluable in various fields such as healthcare, agriculture, food safety, bioprocessing, and environmental monitoring, where they provide accessible and point-of-care diagnostic (POC) solutions.<sup>2,3</sup> For instance, glucose sensors used by diabetic patients and environmental biosensors for detecting pollutants illustrate the impact and utility of biosensors in everyday applications.<sup>4,5</sup> Despite their efficacy, traditional sensor platforms, often reliant on rigid, non-biodegradable materials, face limitations such as high production costs, suboptimal biocompatibility, and challenges in miniaturization and integration into portable devices, particularly for *in vivo* applications, where sample scarcity and tissue integrity are paramount.<sup>6,7</sup> Since the performance and applicability of any biosensor are profoundly influenced by the substrate material upon which the biorecognition layer is immobilized, the ideal substrate should combine mechanical flexibility with the ability

<sup>a</sup>Department of Biotechnology, School of Chemical Engineering, College of Engineering, University of Tehran, Tehran, Iran. E-mail: [mojdeh.mirshafiei@gmail.com](mailto:mojdeh.mirshafiei@gmail.com); [hrashedi@ut.ac.ir](mailto:hrashedi@ut.ac.ir)

<sup>b</sup>Department of Life Science Engineering, Faculty of New Science and Technologies, University of Tehran, Tehran, Iran. E-mail: [amirafshar.ut@gmail.com](mailto:amirafshar.ut@gmail.com); [yazdian@ut.ac.ir](mailto:yazdian@ut.ac.ir)

<sup>c</sup>Department of Physics, University of Zabol, Zabol 9861335856, Iran. E-mail: [a.rahdar@uoz.ac.ir](mailto:a.rahdar@uoz.ac.ir)

<sup>d</sup>Polymat and Department of Applied Chemistry, Faculty of Chemistry, University of the Basque Country UPV/EHU, Paseo Manuel de Lardizabal 3, 20018, Donostia-San Sebastián, Spain. E-mail: [mohammadali.aboudzadeh@ehu.eus](mailto:mohammadali.aboudzadeh@ehu.eus)



to conform to diverse shapes and surfaces while ensuring compatibility with biological environments.<sup>8</sup> Recent investigations have shown that substrate mismatch can significantly impair signal transmission and reduce overall applicability in dynamic environments.<sup>9</sup> Consequently, this has driven significant attention toward nanostructured materials, which offer tunable surface characteristics, high surface-to-volume ratios, and superior signal transduction efficiencies.

Among these, graphene and its derivatives, paper-based matrices, and natural and synthetic polymer films represent the most widely investigated materials, each presenting distinct advantages and trade-offs relevant to biosensing applications. For example, Graphene-based substrates excel in electrical conductivity and sensitivity due to their unique two-dimensional (2D) architecture, yet face challenges such as limited biocompatibility, poor biodegradability, and reproducibility, which restrict their application in biological environments.<sup>10</sup> Paper-based substrates

present an attractive, low-cost, disposable alternative, providing ease of fabrication that makes them ideal for disposable POC diagnostic devices. However, their poor mechanical stability, inconsistent porosity, limited surface uniformity, and reduced biomolecule loading capacity under humid conditions can compromise sensitivity and signal reproducibility.<sup>11,12</sup> Synthetic polymer substrates, such as polyvinylidene fluoride (PVDF) and polyaniline, offer excellent flexibility, conductivity, and processability, along with scalability for industrial fabrication. Nevertheless, their typical lack of a hierarchical nanostructure and their petrochemical origins often lead to poor biocompatibility, biofouling, and inflammatory responses, necessitating extensive surface modifications for biosensing applications.<sup>13–15</sup>

In comparison with other substrate materials, bacterial cellulose (BC) offers a distinctive balance between biocompatibility, sustainability, and functional tunability. As a natural nanostructured polysaccharide biosynthesized primarily by *Gluconacetobacter xylinus*, BC exhibits exceptional purity, ultra-fine fiber network architecture, and remarkable mechanical strength.<sup>16</sup> While native BC lacks certain functional properties such as electrical conductivity, antimicrobial activity, and magnetic responsiveness, these limitations can be effectively addressed through composite formation with conductive polymers, carbon nanotubes (CNT), gold (Au) NPs, graphene oxide, and other functional nanomaterials. Such modifications endow BC with enhanced electrical, optical, and piezoelectric properties, broadening its applicability across diverse sensing modalities.<sup>17–19</sup> Moreover, BC's three-dimensional (3D) porous structure provides an ideal substrate for biosensing applications, offering a large surface area and abundant active sites for the immobilization of enzymes, antibodies, nucleic acids, and other biorecognition elements, thereby facilitating efficient analyte capture and signal generation.<sup>20,21</sup> This unique structure, combined with superior water retention capacity and mechanical flexibility, makes BC particularly suitable for developing wearable and implantable sensors.<sup>17,22,23</sup> Furthermore, BC's innate biodegradability, non-toxic nature, and production capability from renewable agricultural waste feedstocks position it as an environmentally responsible alternative to conventional synthetic materials, addressing growing concerns about electronic waste accumulation from disposable diagnostic devices.<sup>24</sup> Table 1 provides a comparative overview of BC against other common biosensor substrates.

Hybrid BC-based biosensors have unlocked significant potential for advancing electrochemical, optical, and piezoelectric detection technologies. For instance, electrochemical biosensors leverage BC's high surface area and porosity, thereby enhancing biomolecule immobilization and improving sensitivity through the detection of electrical signal variations generated by target-bioreceptor interactions.<sup>25,26</sup> Optical biosensors similarly benefit BC's versatility; its matrix can be chemically modified, for example, through acetylation to achieve optical transparency or functionalization with fluorophores and quantum dots to develop highly responsive systems for monitoring fluorescence and chemiluminescence.<sup>27–29</sup> Similarly, in piezoelectric applications, the inherent mechanical strength of BC provides a robust foundation, where its



Abbas Rahdar

*Dr Abbas Rahdar is an Associate Professor of Nanoscience and Nanotechnology at the Department of Physics, University of Zabol, Iran. In 2017, he was awarded a six-month research fellowship by Iran's Ministry of Science to study polymeric microemulsions for drug delivery at the University of Santiago de Compostela, Spain. His research focuses on nanoparticle synthesis, characterization, and biomedical applications. Dr*

*Rahdar has published over 400 peer-reviewed papers, 15 book chapters, and has ~18 500 citations with an H-index of 68. He has been listed among the world's top 2% scientists by Stanford University for the past four years.*



M. Ali Aboudzadeh

*Dr M. Ali Aboudzadeh is a Ramón y Cajal Fellow at the University of the Basque Country (UPV/EHU), Spain. He earned his PhD in Applied Chemistry and Polymer Materials from UPV/EHU in 2015, following BSc and MSc degrees in Polymer Engineering from Amirkabir University of Technology and Iran Polymer & Petrochemical Institute. He has held multiple postdoctoral positions, including a prestigious Marie Skłodowska-Curie Fellow-*

*ship at CNRS, France, where he developed photoactive core-shell submicron polymer latexes. Author of over 60 publications and editor of two Springer Nature books, his research focuses on polymer synthesis, supramolecular assemblies, rheology, and bioactive compound encapsulation.*

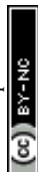


**Table 1** Comparative overview highlighting key parameters of BC, graphene, paper, and synthetic polymers in biosensor applications

Property	Graphene <sup>34</sup>	Paper (plant-derived cellulose) <sup>35,36</sup>	Synthetic polymers (e.g., PDMS, PANI) <sup>15,37–39</sup>	BC <sup>40,41</sup>
Structure	2D sp <sup>2</sup> carbon sheets	Fibrous cellulose sheets	Amorphous/semi-crystalline	3D nanofibrillar network (20–100 nm fibers)
Conductivity	Very high	Insulating	Conductivity varies (e.g., PDMS insulating, PANI: semiconducting (conductivity can be tuned <i>via</i> doping and processing))	Insulating
Biocompatibility/biodegradability	Moderate (ROS risk)/non-biodegradable	High/biodegradable	Varies depending on the polymer; biocompatibility concerns/typically non-biodegradable	Excellent/biodegradable
Mechanical strength (tensile/Young's modulus)	Very high	Moderate	Very low	High
Surface area	Very high	Moderate	Variable	High
Ease of functionalization	High	High	Low-moderate	Very high
Advantages in biosensors	Ultra-high sensitivity and conductivity, large surface area, excellent electron transfer kinetics, facile functionalization, and miniaturizable	Low-cost, easy printing, minimal instrumentation, and portable and disposable (ideal for POC diagnostics)	Flexible fabrication, tunable stability	Low cost, high purity, flexible 3D scaffold for enzyme immobilization, eco-friendly, high porosity for analyte diffusion
Disadvantages in biosensors	High cost, potential cytotoxicity/inflammation, agglomeration in composites, non-biodegradability, scalability and reproducibility issues	Mechanical instability and fragility under humid/wet conditions, limited surface uniformity, lower electrical performance, variability among batches, and limited functionalization density	Hydrophobicity limits cell adhesion, acidic byproducts, and environmental persistence	Requires conductive additives for electrical sensing, variable batch, and functionalization may increase cost/complexity

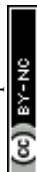
composite structures incorporating NPs such as MnFe<sub>2</sub>O<sub>4</sub> exhibit piezoelectric responses comparable to conventional materials like PVDF, supporting the development of flexible, high-performance mass-sensing platforms.<sup>19,30</sup> This multifaceted compatibility with diverse transduction principles, combined with its sustainability and biocompatibility, firmly establishes BC as an excellent substrate for advanced, high-performance biosensing technologies.<sup>31–33</sup>

In light of the growing demand for sustainable and high-performance biosensing technologies, this review presents the multifaceted potential of BC as a renewable, nanostructured substrate for next-generation analytical devices. It begins by outlining the biosynthetic pathways and distinctive physico-chemical properties that distinguish BC from conventional substrates, emphasizing its suitability for diverse biosensing applications. The discussion then centers on the design of BC-based biosensors, focusing on the integration of biorecognition elements with diverse transduction modalities, including electrochemical, optical, and piezoelectric platforms. Particular attention is given to the expanding applications of BC-based biosensors in healthcare, such as early disease diagnosis, real-time wound monitoring, wearable health tracking, and POC diagnostics, as well as in environmental monitoring and food safety. The discussion concludes by evaluating the convergence of BC-sensors with artificial intelligence and outlining the

persistent challenges and future research avenues that will solidify BC's role in advanced, eco-friendly analytical devices.

## 2. BC

Cellulose stands as the most prevalent, sustainable, and widespread renewable natural polymer on Earth. It forms the structural basis of plant cell walls and is additionally synthesized by certain fungi, algae, and bacteria. Cellulose could be generated through chemical or enzymatic synthesis. Cellulose is a linear polymer consisting of  $\beta$ -1-4-linked D-glucopyranose repeating units.<sup>42</sup> The cellulose chains form elementary sub-fibers through hydrogen bonding, eventually forming microfibrils. The van der Waals forces and hydrogen bonds that hold these saccharide chains together confer high strength, stiffness, durability, and crystallinity to cellulose.<sup>43</sup> Although both plant cellulose and BC are chemically identical, unlike plant cellulose, BC is not associated with hemicellulose, lignin, pectin, and other biogenic products; so it can retain a greater degree of polymerization.<sup>44</sup> Consequently, BC is considered a source of pure cellulose that requires minimal chemical and mechanical treatment and can be easily purified using NaOH solution with low energy consumption.<sup>45</sup> Historically, BC was discovered as a solid mass on fermentation medium surface by Adrian Brown in 1886, when he cultured *Acetobacter* under static conditions.<sup>46</sup>



While *Acetobacter* was the initial strain used to synthesize BC, other bacteria such as *Rhizobium*, *Agrobacterium*, *Azotobacter*, *Pseudomonas*, *Escherichia*, *Salmonella*, *Klebsiella*, *Sarcina ventriculi*, and *Lactobacillus hilgardii* have also been found capable of producing BC.<sup>47,48</sup> Among them, the Gram-negative bacterium *Komagataeibacter xylinus*, formerly known as *Acetobacter xylinum* and *Gluconacetobacter xylinus* stands out as the major strain with high capacity for cellulose synthesis.<sup>49</sup> During BC synthesis, glucose chains generated within the bacterial cell pass through microscopic pores and aggregate to form microfibrils, leading to the formation of cellulose strips. These strips were arranged into a 3D network structure with a highly porous matrix, resulting in a never-dried membrane that retains up to 99% water by weight, making it less prone to microbial attack.<sup>50</sup> The fibers of BC, with nanoscale dimensions ranging from 100 to 1000 nm in length and 10–50 nm in diameter, exhibit remarkable mechanical and physical characteristics.<sup>47</sup>

## 2.1. BC biosynthesis

Cellulose biosynthesis in bacteria serves various purposes, ranging from chemical, mechanical, and physiological stability,

to improving interactions and nutrient diffusion. BC biosynthesis originates in the cytoplasm of bacteria and is carried out in cell membrane, where cellulose synthase polymerizes chemically activated glucose.<sup>51</sup> As shown in Fig. 1, the biosynthesis involves three main steps: (i) uridine diphosphate glucose (UDP-glucose) synthesis: within the bacterial cytoplasm, glucose from the growth medium undergoes a series of enzymatic reactions to transform into UDP-glucose. This conversion is crucial for BC synthesis, as UDP-glucose serves as a key precursor. The tricarboxylic acid (TCA) and pentose phosphate (HMP) cycles provide energy and intermediate metabolites for bacterial growth and cellulose synthesis.<sup>52</sup> (ii) Cellulose chain formation: in the cellular membrane, UDP-glucose is catalyzed by cellulose synthase forming  $\beta$ -1,4 glucan chains. This enzyme complex includes subunits BcsA, BcsB, BcsC, and BcsD, which regulate cellulose synthase activity and yield. The BcsAB subunit catalyzes  $\beta$ -1,4-glucan chains synthesis, while the BcsD subunit aids in crystallization and secretion through BcsC subunits. Moreover, other cofactors like ATP, c-di-GMP, and  $Mg^{2+}$  affect regulating cellulose synthesis.<sup>53,54</sup> (iii) Crystallization and polymerization: after

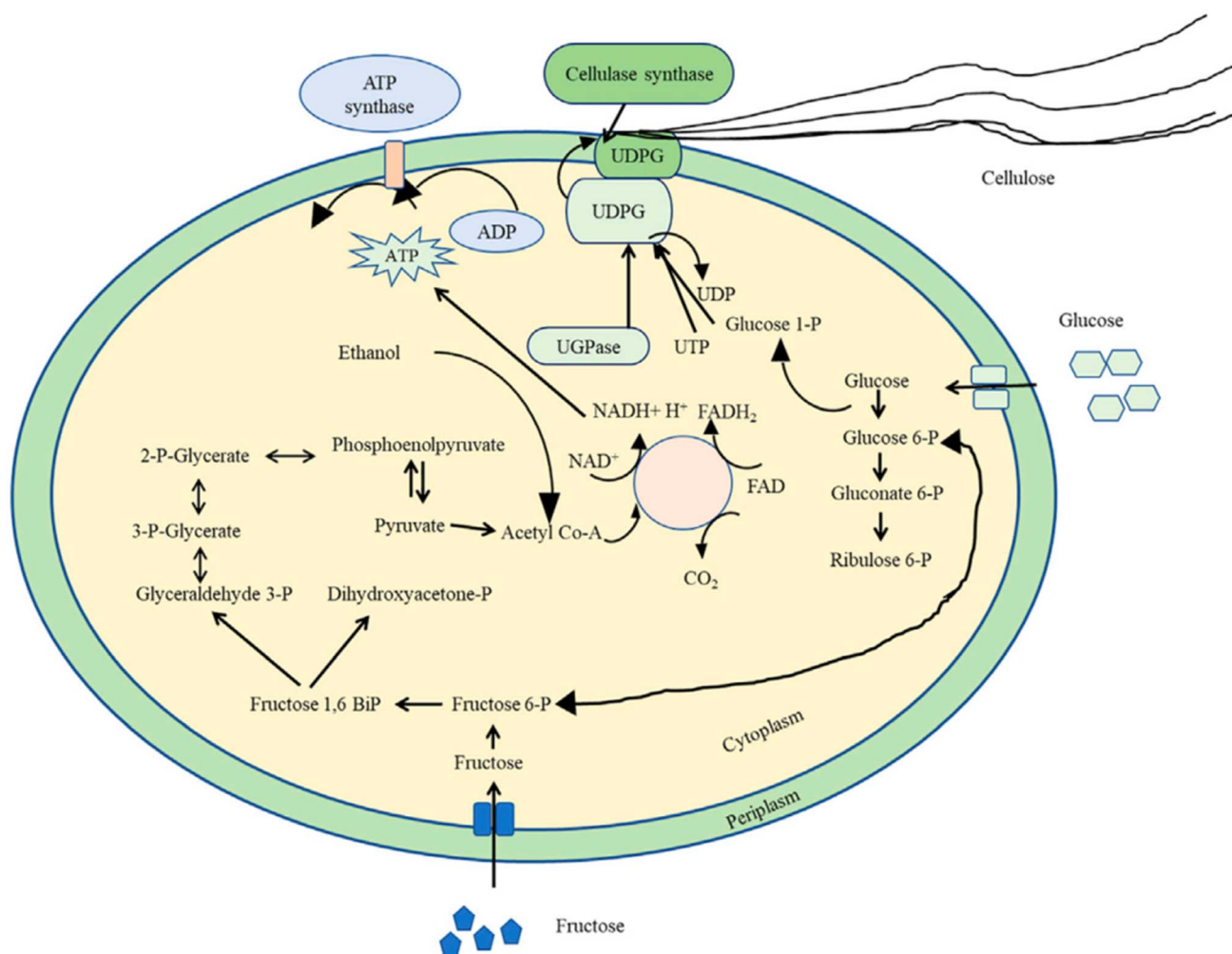


Fig. 1 Schematic representation of cellulose synthesis mechanism. Reproduced with permission from ref. 57 Copyright (2022), Frontiers Media SA.



synthesis, cellulose is secreted from cell membrane. The initial  $\beta$ -1,4-glucan chains form subfibrils through van der Waals forces, regulated by the BcsD subunit. These chains are then discharged through BcsC subunits, functioning like an extruder. The rate of cellulose synthesis is approximately  $2 \mu\text{m min}^{-1}$ , and further bonding occurs outside the cell, elongating the chains.<sup>54</sup> This process ensures the production of bacterial cellulose, which is essential for the bacterium's structural integrity and interaction with its environment. While naturally synthesized bacterial cellulose primarily consists of type I cellulose, the absence of BcsC and BcsD subunits results in the production of shorter, amorphous type II cellulose *in vitro*, though glucan chains are still crystallized and polymerized.<sup>55</sup> During bacterial cell division, both microorganisms continue synthesizing BC, forming branches. Thus, very high degrees of polymerization can be achieved. Moreover, translocation of multiple glucose units typically leads to strand termination, followed by either reinitiation of the released strand or the synthesis of a new strand.<sup>56</sup>

## 2.2. BC properties

BC, a natural, three-dimensional (3D) nanostructure, with eco-friendly properties, derived from bacteria, is considered a cost-effective material employed as a matrix in biosensor design. Its remarkable characteristics, including high purity, biocompatibility, and excellent mechanical strength, make it a compelling alternative to traditional materials.<sup>58–60</sup>

These properties that make it suitable for various analytical and diagnostic purposes are briefly addressed below (Fig. 2).

**2.2.1. High purity and biocompatibility.** BC is produced in a highly pure form, devoid of lignin and hemicellulose, which are typically found in plant-derived cellulose. This exceptional purity significantly enhances both its biocompatibility and hemocompatibility, facilitating seamless integration with biological samples and minimizing the risk of immune responses.<sup>31,61</sup> Such characteristics make BC particularly suitable for medical biosensor applications, where interaction with biological tissues is essential. For example, BC can serve as a skin substitute, routinely used in wound dressings. Its potential as bases for wearable sensors is also noteworthy, as it can address adhesion issues, facilitating skin integration in wearable devices.<sup>31,32</sup> BC's chemical composition and nano-fibrillar structure closely resemble components of the extracellular matrix (ECM), especially collagen, further contributing to its biocompatibility. Additionally, while concerns regarding endotoxins—lipopolysaccharides found in the Gram-negative bacteria outer membrane—are valid, polysaccharide nature of BC helps mitigate potential immunogenic responses associated with these endotoxins.<sup>62</sup>

**2.2.2. Morphological and structural properties.** In biosensor development, a nanostructured polymer refers to a macromolecular material engineered at the nanoscale to exhibit distinctive physicochemical properties arising from its hierarchical organization, such as enhanced surface area,

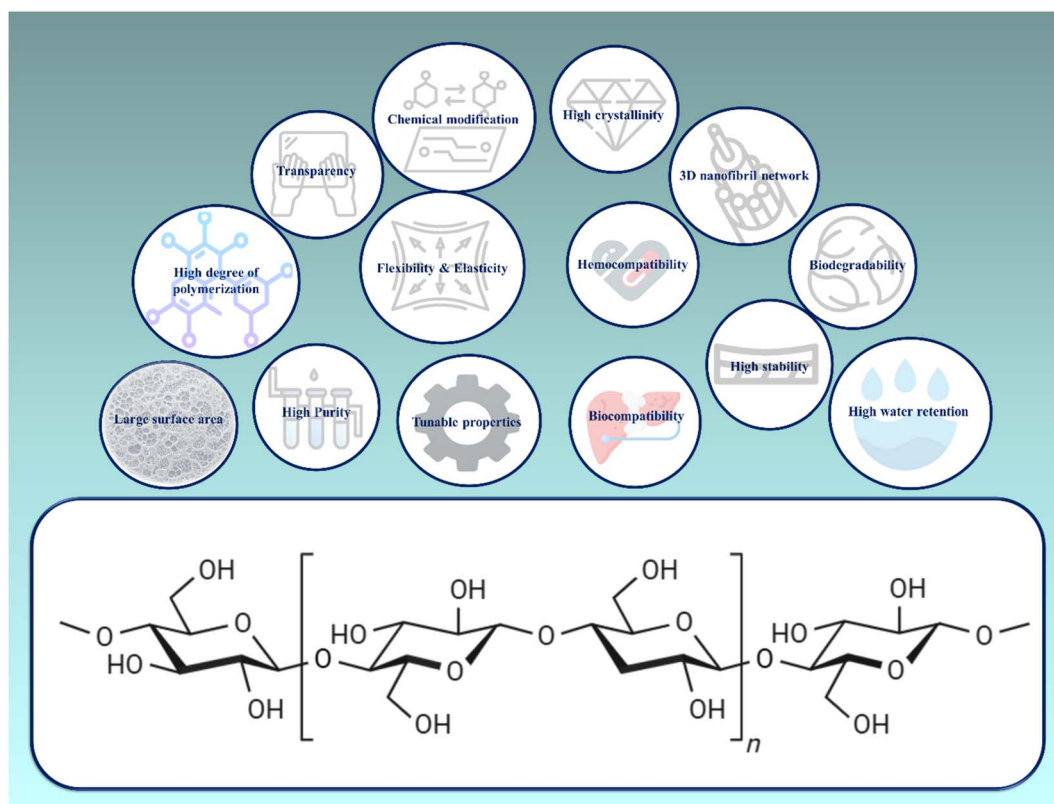


Fig. 2 Schematic representation of BC properties.



porosity, and mechanical integrity. BC exemplifies this class of materials through its unique 3D network of interwoven nanofibers, typically 20–100 nm in diameter, composed of ribbon-like fibrils approximately 2–4 nm wide. This ultrafine reticular architecture imparts BC with exceptional specific surface area, interconnected porosity, and tunable mechanical strength, enabling efficient molecular diffusion and biomolecule immobilization attributes that are critical for biosensing applications.<sup>63</sup> Importantly, BC exhibits tunable porosity, which permits modulation of pore characteristics, including size, spatial distribution, and connectivity, through synthesis variables (e.g., nutrient composition, incubation time) or post-processing methods (e.g., mechanical compression, lyophilization). This tunability allows optimization of analyte transport and interaction with immobilized biorecognition elements, thereby improving sensor sensitivity and response time.<sup>64</sup>

Additionally, owing to its hydrophilic nature, BC can retain up to 90% of its weight in water, providing an ideal microenvironment for maintaining the bioactivity of immobilized molecules. These characteristics facilitate efficient immobilization of biorecognition elements, including enzymes, antibodies, nucleic acids, or aptamers, *via* physical entrapment, covalent bonding, or adsorption, thereby enhancing sensor sensitivity, response time, and overall analytical performance.<sup>65,66</sup> Moreover, BC's structural mimicry of the native ECM, specifically in fiber diameter and porosity, promotes preferential biomolecule adhesion to the cellulose matrix, effectively shielding electronic components from non-specific binding.<sup>67</sup> BC's water retention capabilities further enhance its suitability for biosensing applications, with its capacity to hold water varying from 60 to 700 times its dry weight, depending on synthesis conditions. This property is beneficial for maintaining the activity of immobilized biomolecules and ensuring a stable sensing environment. Moreover, BC's ability to swell in the presence of moisture can improve the diffusion of analytes, thereby increasing the sensitivity of biosensors.<sup>25,41</sup> Other advantageous characteristics of BC include dimensional stability, which is important for piezoelectric sensors,<sup>68</sup> and transparency, a desirable feature for certain types of sensors and electronic devices.<sup>69</sup>

**2.2.3. Mechanical properties.** As expected, BC's mechanical properties are intrinsically linked to its unique structural characteristics. The fibrillar network, lightweight composition, macromolecular properties, and high purity contribute to BC's exceptional mechanical performance. For example, Young's modulus of BC monofilament can reach approximately 114 GPa, with tensile strength values ranging from 200 to 300 MPa. This stress-strain behavior closely resembles that of soft tissues, making BC an excellent reinforcement material for applications requiring high mechanical performance, particularly in the development of both wearable and non-wearable flexible sensors.<sup>19,33</sup> Additionally, its water retention and swelling properties give this biopolymer superior permeability, flexibility, elasticity, and resistance in humid conditions, allowing for the development of robust biosensors capable of withstanding various environmental conditions while maintaining functionality.<sup>70</sup>

Alongside the unique mechanical characteristics of BC, it is important to note that while BC membranes are great at resisting stretching in directions that are parallel to the membrane, they only slightly resist compressive deformation in directions perpendicular to it. BC also possesses high degree of polymerization, reaching up to 10 000, and impressive crystallinity (up to 90%). Crystallinity influences chemical, mechanical, and physical properties; BC comprising both crystalline and amorphous domains. Higher crystallinity in polymers results in stronger polymer chains, increased thermal stability, reduced flexibility, and makes it harder for the chains to break apart. This, in turn, leads to lower moisture absorption and slows down the degradation process. Conversely, a decrease in the crystallinity index can lead to accelerated degradation owing to transforming crystalline regions into amorphous regions.<sup>71</sup>

**2.2.4. Biodegradability.** As a natural polymer, BC is biodegradable, making it an environmentally friendly choice for biosensing applications and aligning with the increasing demand for sustainable materials in technology. While BC can be degraded through enzymatic hydrolysis by cellulase, the human body lacks cellulolytic enzymes, which, combined with BC's high thermal, chemical, and mechanical stability, renders it resistant to biodegradation. This characteristic, however, makes BC suitable for applications requiring long-term support. The degradation rate of BC can be influenced by various factors, such as material parameters (composition and additives presence), morphology, hydrophilicity, pH, crystallinity, molecular weight, and water uptake capacity. To improve its decomposition and biodegradation within biological systems, several strategies have been employed, such as the oxidation of cellulose and the creation of BC composites with cellulose.<sup>31,65</sup>

**2.2.5. Physical modification.** *In situ* synthesis of bacterial nanocellulose (BNC) composites can be challenging due to the influence of additive concentration on cellulose production. *Ex situ* physical methods overcome these limitations by enabling liquids, small solids, or NPs to penetrate or deposit within the porous BNC matrix. Physical methods are classified into coating techniques (e.g., sputtering, thermal evaporation), which allow the deposition of metals and oxides for electronic applications, and impregnation methods (e.g., agitation, vacuum filtration), which facilitate the penetration of functional materials into the nanofibers, forming eco-friendly composites. Although physical methods primarily generate weak interactions (hydrogen bonds, van der Waals, electrostatic, and hydrophobic forces), they effectively promote the immobilization of biomolecules while preserving the BNC's three-dimensional network.<sup>2</sup>

**2.2.6. Chemical modification.** Purifying the initial material is crucial to ensure that cellulose's functional groups are readily accessible for surface interactions with other substances. The high density of hydroxyl groups on surface of BC facilitates its chemical modification. Methods such as phosphorylation, oxidation, and succinylation can alter the molecular structure of BC, creating a favorable environment for chemical modifications that enhance reactive bonding and adjust its physical and mechanical properties. Furthermore, appropriate chemical modifications can enable the covalent immobilization of biomolecules, preventing leaching during sensing analyses and



thereby improving the sensitivity and reproducibility of biosensors. BC can be easily chemically modified to introduce functional groups or NPs, further augmenting its biosensing capabilities.<sup>65,72</sup>

**2.2.7. Tunable properties.** The BC properties could be precisely tailored through manipulating fermentation process and incorporating various functional materials, allowing for customization of the biosensor to meet specific requirements.<sup>73</sup> One inherent advantage of BC is *in situ* moldability, enabling the creation of biosensors in various shapes and sizes, and thicknesses depending on the fermentation conditions used, thereby rendering it well-suited for diverse applications. This adaptability makes BC suitable for a wide range of applications.<sup>72</sup> Recent advancements have demonstrated that BC can be tailored to enhance its electrical conductivity, making it suitable for electrochemical biosensing applications. Conductive composites of BC combined with substances like graphene or carbon nanotubes have been developed to improve signal transduction. By integrating BC with biomolecules and electronic components, a range of flexible, biodegradable, and biocompatible platforms with enhanced electron transfer capabilities have been developed.<sup>60,65</sup>

### 3 BC-based biosensors

A biosensor is an analytical instrument that can convert biochemical reactions into quantifiable signals. The working principle of this system is connected to three primary components: a bioreceptor for biological recognition, a physical-chemical transducer, and an electronic system for signal processing and display (Fig. 3). Biosensors could be classified based on properties of bio-receptors, including antibodies, microbial whole cells, DNA, enzymes, and proteins or fragments. Transducers could also be categorized based on their physico-chemical properties, including thermal, calorimetric, electrochemical, optical, or piezoelectric properties.<sup>74</sup> In the development of biosensors, it is crucial to achieve high biocatalytic activity, selectivity, sensitivity, environmental

compatibility, and cost-effectiveness. BC emerges as a highly advantageous substance for developing biosensors due to its 3D nanostructure, eco-friendly nature, and exceptional properties such as mechanical strength, strong crystallinity, extensive surface area, high absorption capacity, and facile modification and functionalization with NPs, conductive materials, metal oxides, carbon nanotubes, along with biomolecules.<sup>41,75</sup>

#### 3.1. Design and fabrication of BC-based biosensors

The design and fabrication of BC-based biosensors comprise a synergistic integration of biomaterials engineering and analytical sciences, harnessing BC's distinctive nanofibrillar architecture to yield sustainable, biocompatible sensing platforms. This multi-step process commences with the production of high-quality BC, where optimization of growth media and fermentation conditions, such as nutrient composition, pH, temperature, and static/dynamic culturing, tailors the native 3D nanofibrillar network, dictating key properties such as porosity, mechanical strength, and thickness (Fig. 4A).<sup>76</sup> Adjustments during synthesis, including the incorporation of secondary phases or post-formation blending, further refine these properties and transform the nascent BC into a functional scaffold to suit biosensor demands. Once synthesized, BC undergoes purification and processing through methods such as freeze-drying,<sup>77</sup> electrospinning,<sup>78</sup> or 3D printing.<sup>79</sup> These methods enable customization of its morphology, enhancement of surface area, and optimization of porosity, which collectively facilitate improved analyte diffusion and biomolecule immobilization efficiency (Fig. 4B).<sup>65</sup>

The inherent nanostructured organization of BC promotes efficient mass transport and accommodates dense immobilization of diverse biorecognition elements, including enzymes, antibodies, nucleic acids, aptamers, or bacteriophages. These biomolecular receptors enable stereospecific and high-affinity binding to target analytes, initiating quantifiable biochemical cascades or electrochemical responses essential for biosensor operation. Effective immobilization of biorecognition elements is therefore central to biosensor efficacy, ensuring stable,

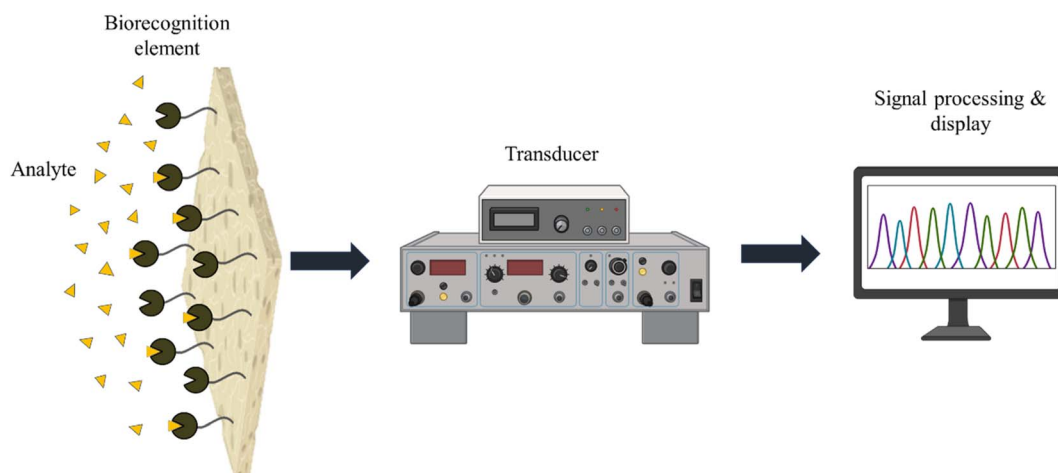
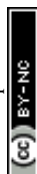


Fig. 3 Schematic representation of a biosensor converting biochemical reactions into quantifiable signals.



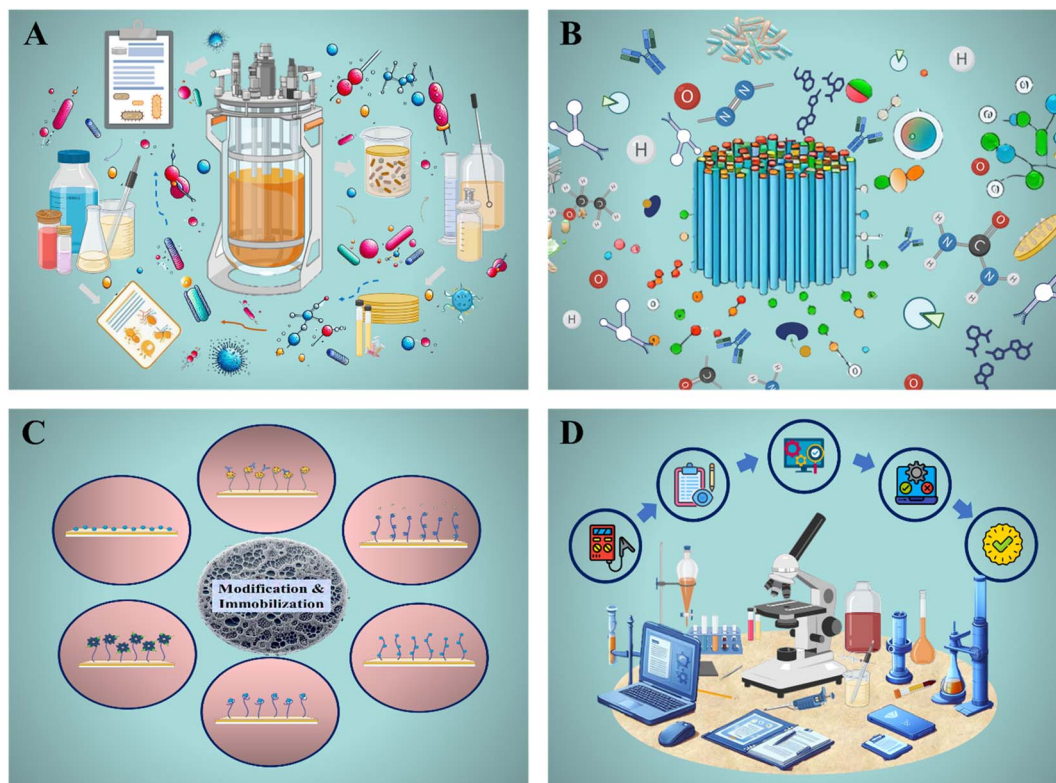


Fig. 4 Design and fabrication of BC-based biosensors. (A) Optimization of the growth medium and fermentation conditions. (B) Modification and functionalization of BC. (C) Immobilization of biorecognition elements. (D) Evaluation and validation.

selective, and reproducible target detection (Fig. 4C).<sup>25,66,80</sup> Immobilization strategies commonly employed in BC-based biosensors include physical adsorption, covalent bonding, affinity interactions, and encapsulation.<sup>81</sup> The choice of technique depends on the type of biorecognition element, desired sensing mechanism, and operational environment.<sup>2</sup> For instance, enzymes such as glucose oxidase (GOx), horseradish peroxidase (HRP), and laccase (Lac) have been successfully immobilized on BC matrices to develop electrochemical biosensors for detecting analytes, including glucose, dopamine, hydroquinone, and hydrogen peroxide.<sup>82</sup> The intrinsic hydrophilicity and nanofibrillar topography of BC create an optimal microenvironment that preserves enzyme conformation and activity, thereby promoting sensor stability and reproducibility over extended periods.<sup>83</sup> Enzyme exemplars include GOx for glucose oxidation to gluconolactone and  $\text{H}_2\text{O}_2$ , HRP for peroxide mediation, and Lac for phenolic substrates like hydroquinone or dopamine; bienzymatic GOx-HRP systems on BC-AuNP scaffolds exemplify cascade amplification. Antibody or phage probes target pathogens, while aptamers, conjugated *via* click chemistry, afford thermal resilience for small-molecule assays. Method selection aligns with biorecognition element stability and transduction needs, ensuring specific analyte capture in complex matrices.<sup>84–86</sup>

The next step involves integrating the BC biosensor with a suitable signal transduction system, which translates analyte-biorecognition element interactions into measurable signals.

Signal transduction mechanisms in BC-based biosensors primarily operate through electrochemical, optical, or piezoelectric principles. Electrochemical transduction remains the most prevalent approach due to its high sensitivity, cost-effectiveness, and compatibility with miniaturized and portable devices. It converts biochemical interactions into measurable electrical signals such as current (amperometry), potential (potentiometry), or impedance (impedimetry), offering rapid, quantitative detection.<sup>40</sup> For example, a BC-based electrochemical sensor integrated with a flexible screen-printed electrode achieved SARS-CoV-2 detection with an ultralow limit of detection (LOD) of  $4.26 \times 10^{-18} \text{ g mL}^{-1}$  and a response time of approximately 10 minutes.<sup>87</sup> In addition, integration of conductive nanomaterials within the BC matrix significantly enhances electron transfer kinetics and reduces detection limits. BC-AuNP, for instance, composites have demonstrated LODs as low as 5.7 nM for hydroquinone, while BC/c-MWCNT/phage systems achieved *Staphylococcus aureus* detection down to 3 CFU  $\text{mL}^{-1}$  within 30 minutes.<sup>88</sup>

Optical transduction mechanisms exploit BC's intrinsic transparency (up to 90% light transmittance) and tunable refractive properties to monitor analyte interactions *via* fluorescence, colorimetry, or surface-enhanced Raman scattering (SERS). In such systems, BC serves as a versatile optical substrate and immobilization matrix for fluorophores, enzymes, or plasmonic NPs.<sup>89,90</sup> Upon analyte binding, alterations in fluorescence intensity or spectral shifts are recorded as





Table 2 Classification of BC-based biosensors based on composite, modification, mechanism, detection target, properties, and application

Composite	B(N)C modification	Sensitive mechanism	Detection target	Detection limit/linear range	Properties	Application	Reference
BNC/Au nanostars/Ag NPs	NP decoration & aptamer-cDNA hybridization	Optical (SERS)	Zearalenone	1.40 pg mL <sup>-1</sup> (10 <sup>-10</sup> pg mL <sup>-1</sup> )	Flexibility, high sensitivity, multiple "hotspot" effects, excellent selectivity, good stability, and reproducibility	Food safety: monitoring ZEN mycotoxin	29
CS-Ag NPs@BC-film + Apt-Au/Fe <sub>3</sub> O <sub>4</sub> NHs	NP decoration & immobilization aptamers	Optical (SERS)	Okadaic acid	2.82 × 10 <sup>-2</sup> nM	Rapid & simplified workflow, high sensitivity & selectivity, and field-deployable potential	Food safety: monitoring of marine toxins	100
Ag@Au NPs-BNC	NP decoration	Optical (SERS)	Thiram	1.412 × 10 <sup>-10</sup> M	Flexible, improved optical sensitivity, reproducibility, and long-term stability	Food safety: pesticide residues detection	18
ZIF67/BC	Immobilization: ZIF67	Electrochemical	Dibutyl phthalate (DBP)	36.63 nM (0–10 μM)	Sustainable & flexible, and good electrical conductivity	Environmental monitoring of plasticizer contaminants	142
Cu MOF@BC	NP decoration	Electrochemical	Bisphenol A	30.5 nM (1–11 μM)	High conductivity, high dispersion, excellent electrocatalytic activity, good stability, selectivity, and reproducibility	Food safety monitoring: Bisphenol A in milk	21
BC@CeZn-MOF	Immobilization: Ce-Zn MOF	Optical: luminescence	Unconjugated bilirubin	0.027 mg dL <sup>-1</sup> (0.1–20 mg dL <sup>-1</sup> )	Luminescent, portable nanopaper, sensitive, smartphone-readable, and reversible photophysical behaviour	POC neonatal jaundice screening (clinical diagnostics)	97
BC/c-MWCNTs	Immobilization: phage	Electrochemical (amperometry)	<i>S. aureus</i>	—	High sensitivity and selectivity, fast response, and biocidal activity	Food safety: early detection of <i>S. aureus</i> in food samples, including milk	129
BC/N-CDs	QD: N-CDs	Optical: fluorescence-based	Fe <sup>3+</sup>	84 nM/(0.5–600 μM)	Biocompatibility, high sensitivity, and sustainability	Environmental monitoring: Fe <sup>3+</sup> detection in aqueous solution	143
BC/Pd NPs/Lac	Enzyme: Lac	Electrochemical (amperometry)	Dopamine	1.26 μM/(5–167 μM)	Excellent stability, reproducibility, and repeatability, wide linear range, low detection limit, high selectivity, high sensitivity	Dopamine detection in clinical samples	144
BC/Au NPs/Lac	Enzyme: Lac	Electrochemical (amperometry)	Hydroquinone	5.71 nM/(30–100 nM)	High sensitivity, low detection limit, wide linear range, excellent stability, good repeatability, and reproducibility	Hydroquinone detection in water environments	145



Table 2 (Contd.)

Composite	B(N)/C modification	Sensitive mechanism	Detection target	Detection limit/ linear range	Properties	Application	Reference
BC/ZnO	Dposition: ZnO	Optical	NO <sub>2</sub> Acetone Ethanol	—	Good response, eco-friendly, biocompatibility, thermal stability, low thickness, stretchability, and cost-effective	Environmental monitoring: gas sensor	146
BC/c MWCNTs/ZIF-8@LAC	Encapsulation: Lac	Electrochemical (amperometry)	Bisphenol A	$1.95 \times 10^{-3}$ mM/ (0.01–0.4 mM)	High flexibility, excellent power density, linear dynamic range, low detection limit, and self-powered ability	Environmental monitoring: water pollutant detection	147
BC/PPy/TiO <sub>2</sub> -Ag	Polymerization: PPy	Electrochemical (conductometric)	<i>E. coli</i> <i>S. aureus</i> <i>S. aureus</i> <i>A. hydrophyla</i> BOD	—	Short response time, portability, high sensitivity, and simple fabrication	A diagnostic instrument developed to boost biological safety	128
BC/ <i>S. cerevisiae</i> -menadione/KB	Immobilization: <i>S. cerevisiae</i>	Electrochemical (amperometry)		10 to 220 mg O <sub>2</sub> per L	Wide linear range, rapid response time, and reliable operational stability	Environmental monitoring: assessing organic pollution in water	148
BC/CdTe	QD: CdTe wet spinning	Optical: fluorescence-based	Glucose	0.026 mM	High and adjustable sensitivity	Developing wearable sensing devices	116
BNC/chitosan-chondroitin sulfate bilayer	Immobilization: P53 antigen	Electrochemical	P53	0.16 U mL <sup>-1</sup> / (0.01–1000 U mL <sup>-1</sup> )	Cost-effective with high sensitivity and selectivity	Diagnostics: early detection of cancer cells	102
BNC	Enzyme: lactate oxidase	Electrochemical (amperometry)	Lactate	4.38 mmol L <sup>-1</sup> / (1.0 to 24.0 mmol L <sup>-1</sup> )	Mechanical flexibility, biocompatibility, and linear response range	Wearable devices	26
BC/PVAN (polyvinylaniline)/PAni	PVAN/PANI bilayer	Electrochemical (amperometry)	Neural stem cell (NSCs)	21 Ω, 39 μF	High electrical conductivity and biocompatibility	Detecting or stimulating neural differentiation of NSCs	149
BC/MXene (Ti <sub>3</sub> C <sub>2</sub> )	Integration: Ti <sub>3</sub> C <sub>2</sub>	Piezoelectrical	Pressure	(0–10 kPa)	High sensitivity, low detection limit, linear sensitivity, as well as ultrahigh compressibility and elasticity	Wearable electronic devices	150
BC/Cr	Embedding: Cr	Optical	Human serum albumin	(25–400 μM)	Portability, affordability, simplicity, efficiency, and eco-friendly	Optical biosensing	151
BC/Au NPs/ionic liquid	Ionic liquids	Optical	Water-glycerin	13.54 a.u./7.4 × 10 <sup>-5</sup> RIU	Simple structure, cost-effective, eco-friendly, versatility, and good sensitivity	Biochemical sensing	152
BC-MWCNTs	Supercritical CO <sub>2</sub> method	Piezoelectrical	Strain	21 GF	Flexible and light weight	Human motion detection	153



Table 2 (Contd.)

Composite	B(N)/C modification	Sensitive mechanism	Detection target	Detection limit/ linear range	Properties	Application	Reference
BC/graphene/Lac	Immobilization: Lac	Electrochemical (amperometry)	Catechol	0.085 $\mu\text{M}$ /(0.2 to 209.7 $\mu\text{M}$ )	High selectivity, wide linear response range, fast response time, and low limit of detection	Environmental monitoring: water pollutant detection	154
BC-ZIF8	Immersion: ZIF8	Electrochemical	$\text{Pb}^{2+}$ $\text{Cd}^{2+}$	390 $\text{mg g}^{-1}$ 220 $\text{mg g}^{-1}$	Exhibiting low density, hierarchical pore structure, excellent adsorption performance large surface area, and high efficiency in mass transfer	Environmental monitoring: heavy metal detection	155
BC/PEDOT:PSS	Impregnation: ILs	Resonant	Mass	3.5 mg	High sensitivity, flexibility, eco-friendliness, and affordability	Mass sensor	156
BC/TEMPO/CDS	QD: CDS	Optical	Photoluminescence modulating compounds	—	pH stability	Biosensing	157
BC/Lac/MWCNTs/AuNPs	Immobilization: Lac GOx	Electrochemical (amperometry)	Glucose	$2.874 \times 10^{-3}$ mM/(0–50 mM)	Broad linear dynamic range, high sensitivity, high power density, and excellent flexibility	Self-powered biosensors and wearable devices	4
CBC- $\gamma$ -AlOOH		Electrochemical	$\text{Cd}^{2+}$ $\text{Pd}^{2+}$	0.17 $\mu\text{g L}^{-1}$ /(0.5–250 $\mu\text{g L}^{-1}$ ) 0.10 $\mu\text{g L}^{-1}$ /(0.5–250 $\mu\text{g L}^{-1}$ )	High sensitivity and selectivity, along with low detection limit	Environmental monitoring: heavy metal detection	158

analytical signals, enabling real-time, label-free detection. For example, BC/AuNP-based SERS platforms have been developed for pesticide detection with a LOD of 0.24 ppm ( $\sim 1 \mu\text{M}$ ), demonstrating the high optical sensitivity achievable through nanoplasmonic enhancement within the BC framework.<sup>90</sup> Piezoelectric transduction relies on the generation of electrical charges from mechanical stress or mass-induced frequency shifts in piezoelectric materials such as quartz crystal microbalance (QCM), ideal for label-free, real-time monitoring of adsorption events. When integrated with BC composites, particularly conductive hybrids incorporating graphene oxide or metallic NPs, these systems convert minute mass changes into electrical signals with exceptional sensitivity, achieving femtomolar-level detection limits.<sup>91,92</sup>

To achieve high signal fidelity, BC is often functionalized with nanomaterials or conductive polymers that facilitate electron transfer and enhance the sensitivity of signal transduction. Incorporating metallic NPs, metal oxides or conductive polymers not only surmounts BC's native insulation but also enhances its catalytic activity and surface reactivity. This synergistic combination within BC nanocomposites significantly improves the signal-to-noise ratio and amplifies the biosensor response.<sup>93–95</sup> Finally, the BC-based biosensor undergoes rigorous testing and validation to ensure its performance and reliability (Fig. 4D). Assessing performance metrics, including sensitivity, selectivity, response time, detection limit, and stability under various conditions, guarantees the biosensor's accuracy and reliability in real-world applications.

### 3.2. Application of BC-based biosensors

Biosensors have attracted considerable interest in recent years owing to their strong capability to detect various analytes. They are categorized into healthcare biosensors, environmental monitoring biosensors, and food safety biosensors. Table 2 presents an overview of recent developments in BC-based biosensors, highlighting their composites, surface modifications, detection mechanisms, target analytes, key properties, and applications.

**3.2.1. BC-based biosensors in healthcare.** In response to increasing demand for rapid, accurate, decentralized, and efficient healthcare monitoring, biosensors have garnered significant interest in medical research. The highly porous structure of BC can promote rapid analyte diffusion, thereby directly impacting key biosensor performance. This is quantifiably demonstrated through enhanced LOD and faster response times, which underpin the platform's high sensitivity and suitability for real-time monitoring.<sup>33,96</sup> This section explores the diverse applications of BC-based biosensors in healthcare, focusing on their roles in early disease diagnosis, wound healing and infection monitoring, wearable and POC devices.

**3.2.1.1. Early disease diagnosis and biomarker detection.** Early disease diagnosis critically depends on the rapid and precise detection of biomarkers. BC-based biosensors provide a highly sensitive and stable platform owing to their porous nanofibrillar architecture, which facilitates efficient analyte diffusion and effective immobilization of biorecognition

elements. Leveraging their high surface area and exceptional biocompatibility, BC-based biosensors have significantly advanced early disease detection through enhanced biomarker sensitivity.<sup>97</sup> The incorporation of enzymes, antibodies, or nucleic acids within BC matrices enables the detection of trace-level disease biomarkers, surpassing conventional rigid sensor substrates in both selectivity and response time. The operational principle of these biosensors is based on converting biological interactions into quantifiable signals, achieved through the integration of biological recognition elements with a transducer. Upon specific binding of the target analyte, the transducer output changes, allowing precise measurement. These devices typically employ electrochemical, optical, or impedance techniques to transduce specific analyte binding into measurable signals, enabling detection at picogram levels in complex biological matrices such as serum or saliva.<sup>98,99</sup> Moreover, these systems can modulate and monitor biological signals in real time within living organisms, allowing for controlled release or detection of proteins and antibodies in response to physiological conditions such as tissue injury, inflammation, infection, cardiac infarction, or muscular dystrophy.<sup>16,100</sup> These sensors provide several advantages compared to traditional diagnostic methods, such as faster turnaround times, higher sensitivity, and lower sample volumes.<sup>41</sup>

For instance, Wu *et al.* designed the two-dimensional (2D) bacterial cellulose nanogold substrate for sensitively detecting tumor necrosis factor- $\alpha$  (TNF- $\alpha$ ). This sensor achieved the notable detection limit of  $0.35 \text{ pg mL}^{-1}$ , demonstrating its high sensitivity and potential for early cancer screening.<sup>101</sup> Similarly, an interdigital BC immunosensor targeted the p53 antigen in MCF-7 breast cancer cell lysates, yielding an LOD of 0.16 U cell per mL *via* impedance spectroscopy, which was directly correlated with tumor progression for noninvasive screening.<sup>102</sup> Optical enhancements further boost sensitivity; for example, a silver nanoparticle-decorated BC membrane (Ag NPs-BCM), fabricated *via* silver mirror reaction and shrinkage, generates uniform Surface-Enhanced Raman Spectroscopy (SERS) hot-spots. This platform detected the cancer-associated redox biomarker glutathione (GSH) at concentrations as low as  $0.1 \mu\text{M}$  in serum, enabling high-sensitivity cancer profiling from minimal sample volumes.<sup>103</sup> Moreover, BC-based biosensors provide an effective solution for rapid and accurate detection of infectious diseases, particularly in the context of preventing and controlling outbreaks. Their suitability for frequent POC testing is highlighted by Lima *et al.*'s development of a simple and portable electrochemical biosensor for SARS-CoV-2 detection. This sensor achieved ultrasensitive results (requiring only 10 mL of nasopharyngeal/oropharyngeal (NP/OP) sample and delivering results within 10 minutes) with high reproducibility (RSD = 3.78%) and selectivity.<sup>87</sup>

**3.2.1.2. Wound dressings and infection monitoring.** BC has long been recognized for its exceptional wound-healing properties, attributed to its excellent moisture retention, gas permeability, and non-toxicity. These characteristics not only support the healing process but also provide an ideal substrate for engineering advanced "smart" wound dressings. By



integrating biosensing capabilities, BC is being transformed from a passive covering into an active monitoring system that can monitor the wound microenvironment, including pH, specific proteases, and biomarkers such as cytokines, in real time to facilitate precision wound management. Highly sensitive electrochemical biosensors, in particular, show great potential for real-time biomarker monitoring in wound exudate, offering improved diagnostic and therapeutic outcomes.<sup>104–106</sup> Nevertheless, conventional biosensors often face challenges with biofouling in the complex environment of wound exudate. To address this, Lv and colleagues designed a novel antifouling electrochemical biosensor for detecting involucrin, a key wound healing marker. Their approach utilized a wound dressing comprised of a composite hydrogel formed by oxidized BC (OxBC) and quaternized chitosan (QCS). Through careful optimization of the OxBC/QCS ratio, the hydrogel achieved electrical neutrality and enhanced hydrophilicity, imparting exceptional antifouling and antimicrobial properties. This biocompatible hydrogel served as a platform for immobilized involucrin antibody SY5, resulting in a biosensor with linear detection (range from  $1.0 \text{ pg mL}^{-1}$  to  $1.0 \text{ }\mu\text{g mL}^{-1}$ ) and low detection limit ( $0.45 \text{ pg mL}^{-1}$ ). Importantly, the biosensor demonstrated high accuracy in detecting involucrin in real wound exudate samples. The antifouling and antimicrobial characteristics of the OxBC/QCS hydrogel not only prolonged the biosensor's functional lifespan but also ensured reliable and consistent sensing performance.<sup>25</sup>

Further advancing BC's role in wound management, Yang and Choy developed a pH sensor for chronic wounds utilizing

a conductive 3D carbon nanofiber aerogel derived from pyrolyzed BC. This sensor, combined with a flexible and proton-selective composite, exhibited remarkable pH sensitivity, enabling continuous pH monitoring and early infection detection.<sup>107</sup> Similarly, Eskilson *et al.* demonstrated the integration of pH sensing capabilities into BC-fabricated hydrogel-based wound dressings. By encapsulating a pH-responsive dye (bromothymol blue) within mesoporous silica nanoparticles (MSNs) incorporated into BC (Fig. 5A and B), they developed wound dressings capable of pH monitoring continuously with precise spatiotemporal resolution (Fig. 5C and D). The dressings exhibited distinct color changes at low pH levels, transitioning to highly contrasting color upon the pH exceeded 6 (the critical range for detecting wound infection) (Fig. 5E and F). This innovation enabled real-time monitoring of wound conditions, facilitating early diagnosis and treatment of infections, ultimately reducing complications and supporting optimal wound healing.<sup>108</sup>

Furthermore, BC holds immense potential for enhancing wound healing through strategic modifications. Incorporating bioactive agents, such as growth factors, antimicrobial peptides, or anti-inflammatory drugs, into the BC structure can promote specific aspects of wound healing, accelerating the healing process. This targeted approach allows for the development of sophisticated wound dressings that address various challenges associated with wound management.<sup>109</sup> Researchers have also explored the integration of BC with advanced materials such as metal–organic frameworks (MOFs) to develop biomimetic nanoreactors capable of addressing specific

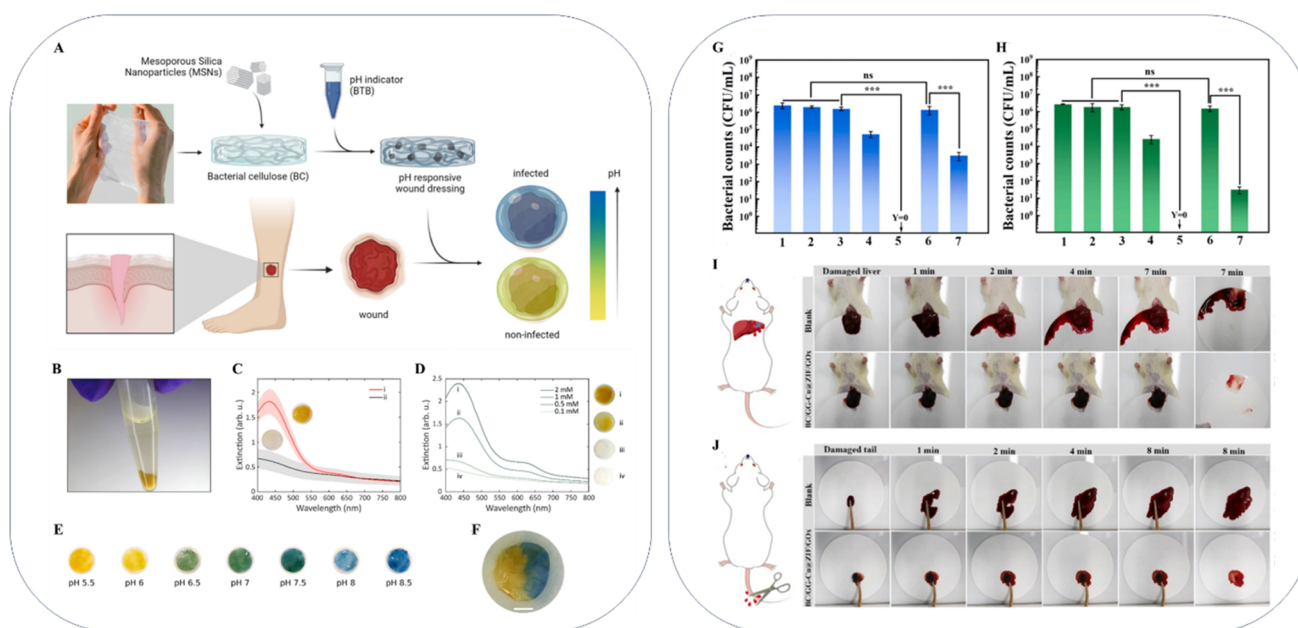
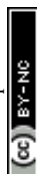


**Fig. 5** BC-based biosensors for wound dressings and infection monitoring. (A) Schematic representation of the fabrication of pH-responsive nanocomposite wound dressings by impregnating BC with MSNs loaded with a pH-sensitive dye (bromothymol blue, BTB) and functionalized with polyethyleneimine (PEI). (B) Photograph of MSN-BTB-PEI. (C) Schematic illustration of pH@BC synthesis methods. (D) BTB concentration effect on color intensity. (E) Color change of pH@BC at pH 5.5–8.5. (F) Image demonstrating spatial pH sensing using the dressing (scale bar: 2 mm). Reproduced with permission from ref. 108. Copyright (2023), Elsevier Ltd. (G) Antibacterial efficacy against *S. aureus*. (H) Antibacterial efficacy against *E. coli*. (I) Schematic and photographs of the mouse liver hemorrhage model. (J) Schematic and photographs of the mouse tail amputation model. Reproduced with permission from ref. 110. Copyright (2022), Elsevier Ltd.



healthcare needs. A notable example is the hybrid hydrogel system composed of BC and guar gum (GG) encapsulating a Cu@ZIF/glucose oxidase (GOx) nanoreactor. This system demonstrated potent antibacterial activity by consuming glucose and generating highly oxidative radicals, effectively eliminating bacterial infections (Fig. 5G and H). Additionally, its high water absorption capacity effectively controlled hemorrhage through blood absorption and activation of coagulation cascades (Fig. 5I and J).<sup>110</sup> The combination of BC with metal NPs forms nanocomposites that exhibit exceptional properties for various applications. While traditional methods often limit control over NP concentration, shape, size, and surface chemistry, a novel self-assembly strategy has been developed to fabricate well-defined BC-NP composites with colloidal silver and gold NPs. This method enables the creation of nanocomposites with unique optical and biophysical properties, opening doors for advanced wound care and biosensing applications. Furthermore, integrating plasmonic gold NPs uniformly into BC enables the modulation of optical properties through mechanical stimuli. This unique mechanoplasmonic effect leads to tunable spectral variations and improved broadband absorption, facilitating novel biosensing strategies.<sup>111</sup> Integrating these multifunctional nanocomposites into wound dressings enables the real-time monitoring of healing dynamics, facilitating more effective interventions and improved patient outcomes.

#### 3.2.1.3. Wearable sensors for continuous health monitoring.

The advancement of wearable biosensors for continuous, non-invasive monitoring relies on finding materials that combine electronic functionality with patient comfort. BC's unique combination of flexibility, transparency, and natural skin adhesion allows for the fabrication of soft, skin-conformal sensors that provide high comfort and durability. The biocompatibility, breathability, and semi-permeability of BC ensure long-term wear without irritation, while its porous nanofibrillar structure supports the integration of conductive fillers for sensitive and responsive signal detection. Moreover, BC's renewable and hypoallergenic nature promotes sustainable, long-term applications, establishing it as a superior platform for next-generation wearable biosensors designed for continuous health monitoring and early disease detection. Current clinical monitoring instruments often face limitations associated with rigid packing, cumbersome wiring, and bulky devices necessitating cumbersome straps or adhesives for skin mounting.<sup>65,112</sup> In this regard, Silva *et al.* developed a novel, non-invasive method for monitoring body fluids, specifically sweat, using microbial nanocellulose sheets as skin-like platforms. These platforms, equipped with screen-printed carbon electrodes (SPCEs), effectively detected toxic metals such as cadmium ( $\text{Cd}^{2+}$ ) and lead ( $\text{Pb}^{2+}$ ) with high sensitivity. This research highlighted the potential of BC-based wearable sensors for real-time monitoring of environmental exposures and early warning of potential health risks.<sup>112</sup>

BC-based biosensors hold substantial promise for advancing wearable technology and human-computer interaction (HCI). Their capacity to precisely sense a spectrum of human motions, from subtle physiological signals such as vocalizations,

respiration, and pulse waves to more pronounced activities, renders them exceptionally suitable for seamless integration into textile substrates. This functionality underpins the creation of sophisticated HCI systems, enabling intuitive and responsive interfaces between users and machines.<sup>77</sup> In a representative study, Gao and colleagues engineered a biodegradable, flexible strain sensor leveraging BC for advanced human-interactive applications (Fig. 6). The fabrication process entailed *in situ* modification of BC during microbial fermentation, incorporating polypyrrole (PPy) NPs directly into the evolving fibrillar network of BC. Subsequent encapsulation with the biocompatible elastomer Ecoflex (EF) yielded a robust BC/PPy@EF composite, bolstering mechanical durability and extensibility while preserving the intrinsic 3D reticular architecture of BC. This structural design conferred exceptional sensitivity through mechanisms involving fibril alignment and fracturing of conductive networks under applied strain. The resulting sensor exhibited outstanding performance metrics, including an ultralow strain detection limit of 0.05%, a broad operational range extending to 90% strain, and a high gauge factor spanning 3.21–4.86. It reliably captured nuanced movements (0.05–1% strain, *e.g.*, respiration and pulse) as well as vigorous actions (up to 90% strain, *e.g.*, squatting and walking). Moreover, the device demonstrated robust long-term stability, with no discernible degradation in sensitivity following 1000 cycles of 90% strain, a resilience attributed to the synergistic effects of EF encapsulation and the inherent tensile strength of the BC matrix. As depicted in Fig. 6, the sensor enabled real-time monitoring of diverse body motions, including finger bending (Fig. 6A), vital signs such as pulse and respiration (Fig. 6B), wrist and elbow flexion using armband configurations (Fig. 6C and D), and knee movement detection *via* a kneecap sensor (Fig. 6E). Additionally, wearable textile integrations (Fig. 6F–H) facilitated tracking of wrist pulse, breathing rate, and throat vibrations. The practical application of the sensor was demonstrated through its integration into a smart glove (Fig. 6I), where five sensors at the knuckle joints enabled real-time gesture recognition (Fig. 6J). The system successfully distinguished ten different numerical gestures with 99.2% accuracy, allowing a robotic counterpart to replicate the human gestures. This achievement highlights the transformative potential of BC-based biosensors in facilitating precise and reliable HCI applications.<sup>113</sup> The adaptability of BC in wearable formats positions it as a key enabler for next-generation electronic skin (e-skin) technologies, capable of continuously monitoring physiological signals such as pulse, respiration, sweat composition, and mechanical strain with high precision.<sup>33,114</sup>

**3.2.1.4. POC testing and personalized medicine.** POC biosensors aim to deliver rapid, accurate, and user-friendly diagnostics outside traditional laboratory environments. The unique properties of BC, including its biocompatibility, flexibility, and ease of fabrication, make it particularly suitable for POC platforms that demand flexibility, miniaturization, and cost-effectiveness. These sensors process minimal samples with high reproducibility, enabling timely diagnosis and treatment interventions, particularly in non-laboratory settings.<sup>26,87,115</sup> Their detecting ability of specific biomarkers associated with individual



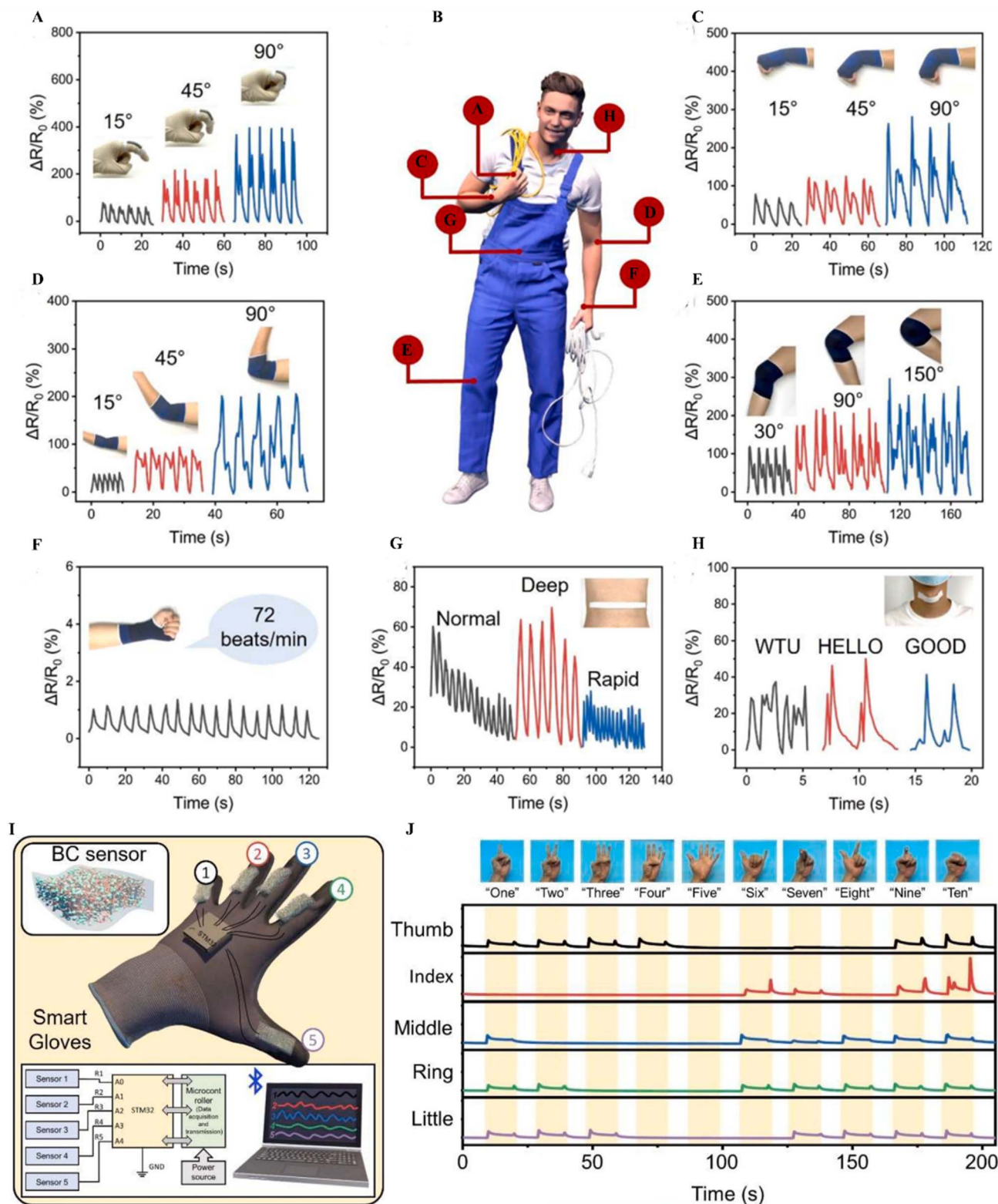
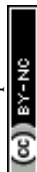


**Fig. 6** BC-based strain sensors (BC/PPy@EF) for full-range body motion detection and human–computer interaction. (A) Sensor output during finger motion. (B) Sensor placement for vital sign monitoring. (C and D) Armband for wrist and elbow bending detection. (E) Kneecap sensor for knee flexion detection. (F–H) Wearable textiles for monitoring wrist pulse, breathing rate, and throat vibration. (I) Schematic illustration of the working principle of wearable smart glove integrated with a BC/PPy@EF sensor network for gesture recognition. (J) Real-time normalized resistance signals for gesture recognition. Reproduced with permission from ref. 113. Copyright (2023), Elsevier B.V.



patients' conditions, such as urine, saliva, and blood, alongside real-time patient data, paves the way for home-based chronic disease management and personalized treatment plans. This approach, known as precision medicine, has great potential to enhance patient outcomes and optimize healthcare delivery.<sup>65</sup> For example, BC biosensors demonstrate superior accuracy, sensitivity, and long-term stability compared to conventional methods for glucose monitoring in diabetes management. Studies have shown that BC-based colorimetric pH sensors exhibit rapid response and a wide linear range, while BC/carboxymethyl cellulose (CMC)-based colorimetric glucose sensors offer low detection limits and high accuracy, making them suitable for non-invasive on-skin health monitoring.<sup>99</sup> In another study, wet-spinning of CdTe quantum dot (QD)-loaded BCnanofibers yielded color-tunable luminescent macrofibers, enabling the creation of fiber-based structures with tunable green, yellow, and orange fluorescence through size control of the QDs. These fibers exhibited sigmoidal pH sensitivity and high glucose sensitivity.<sup>116</sup> These examples highlight BC-based biosensors' potential to revolutionize healthcare by enabling personalized treatment plans and optimized disease management strategies.

### 3.2.2. BC-based biosensors in environmental monitoring.

In environmental monitoring, biosensors have achieved significant success in detecting and monitoring heavy metals and other harmful substances in water and soil. These devices offer a sensitive and eco-friendly approach, providing valuable data for environmental protection and management. Specifically, BC-based biosensors can detect various pollutants, including organic contaminants, metals, bacteria, and pharmaceuticals. This capability allows for real-time insights, enabling timely intervention measures.<sup>2,117</sup> BC-based biosensors can immobilize metal-binding proteins or aptamers that specifically bind to heavy metals. This interaction can be detected electrochemically, resulting in the development of highly sensitive and selective biosensors for monitoring heavy metal pollution in water and soil.<sup>2,41</sup> Unlike traditional sensors, these biosensors require no electronic components, sophisticated equipment, or trained personnel, making them more accessible and practical for widespread use.<sup>118</sup>

Recent advancements in this field have focused on enhancing their effectiveness in detecting and monitoring heavy metals. For instance, Parizadeh *et al.* developed a platform that efficiently detects Cu(II) ions quickly, easily, and affordably through an effective and green metallochromic sensor by embedding anthocyanin derived from the peels of black eggplant in BC nanofibers. This sensor detected Cu(II) ions quantitatively in solid and solution states, exhibiting detection limits of 20–300 ppm and 10–400 ppm, respectively. In aqueous matrices, the sensor operated within a pH range of 3.0 to 11.0, demonstrating the visual colorimetric response to Cu(II) concentration, changing from brown to light blue and dark blue.<sup>118</sup> In another study, BC was utilized as the structural framework for BC/GO/polyvinyl alcohol/attapulgite (BC/GO/PVA/APT) composites to adsorb Cu<sup>2+</sup> and Pb<sup>2+</sup> ions from solutions. The results demonstrated that this hydrogel possesses superior hydrophilicity, enhanced thermal stability, and a large

specific surface area compared to conventional materials. The Freundlich kinetic effectively modeled the adsorption of Cu<sup>2+</sup> (150.79 mg g<sup>-1</sup>) and Pb<sup>2+</sup> (217.8 mg g<sup>-1</sup>) ions.<sup>119</sup>

Effective heavy metal ion removal from industrial wastewater remains a significant challenge in water treatment. Estimating bioavailable heavy metals is crucial for assessing ecological risks.<sup>120,121</sup> Thus, a cost-effective and mini-equipment biosensing process to detect heavy metals in water, providing insights into their bioavailability and cytotoxicity.<sup>122</sup> BC-based biosensors show great promise for monitoring water quality. For example, Deshpande *et al.* developed an innovative electrochemical sensor based on a composite of ascorbic acid-functionalized silver NPs (AsAgNPs) embedded within a nanocrystalline BC (NBC) matrix for the ultrasensitive detection of Hg<sup>2+</sup> ions in water (Fig. 7A). The AsAgNP-NBC matrix enhanced mercury sensing by forming water-insoluble complexes capable of binding and reducing Hg<sup>2+</sup>, thereby enabling highly sensitive electrochemical detection through cyclic voltammetry (CV) and differential pulse voltammetry (DPV). As indicated in Fig. 7B, under light irradiation (455 nm), the screen-printed electrode (SPE) demonstrated a 1.9-fold photocurrent enhancement, achieving an ultralow detection limit of 3.95 pM (CV) and 2.717 pM (DPV) within a linear range of 25 pM–50 nM (Fig. 7C and D). Selectivity tests confirmed strong specificity for Hg<sup>2+</sup> over other metal ions (Fig. 7E), highlighting the potential of this light-activated nanocomposite for achieving ultra-trace level detection of environmental contaminants.<sup>123</sup> On the other hand, BC-based biosensors facilitate the development of miniaturized, portable systems for on-site effluent monitoring. A recent study demonstrated the successful *in situ* synthesis of freestanding nanopapers from Zr-MOF grown on BC, forming BC@Zr-MOF (Fig. 7F). This composite exhibits selective recognition and enrichment of dichromate ions (Cr<sub>2</sub>O<sub>7</sub><sup>2-</sup>) in water, with a notable adsorption capacity (90 mg g<sup>-1</sup>). The sensing mechanism, schematized in Fig. 7G, relied on the fluorescence quenching of the BC@Zr-MOF in the presence of the target analyte. This allowed for rapid and sensitive detection, as shown in Fig. 7H, where the emission intensity decreased progressively with increasing Cr<sub>2</sub>O<sub>7</sub><sup>2-</sup> concentration, achieving a low LOD of 6.9 nM. Furthermore, the practical utility of the sensor was confirmed by its stable fluorescence response across a wide range of pH values (Fig. 7I), underscoring its robustness for environmental monitoring applications.<sup>124</sup>

**3.2.3. BC-based biosensors in food safety.** Ensuring the quality and integrity of the food supply is paramount in food safety, particularly given the ever-present threat of foodborne pathogens, chemical residues, and spoilage, which can cause illness and even death. Traditional analytical techniques, while accurate, are often time-consuming, labor-intensive, and require centralized laboratories, limiting their utility for rapid, on-site decision-making. In contrast, a new generation of biosensors based on BC is emerging as a robust solution for enhancing food safety. The high purity, biocompatibility, and excellent mechanical strength of BC provide a stable and reliable platform for immobilizing biorecognition elements, such as enzymes or antibodies, which are essential for the detection of specific foodborne pathogens.<sup>2,125</sup>



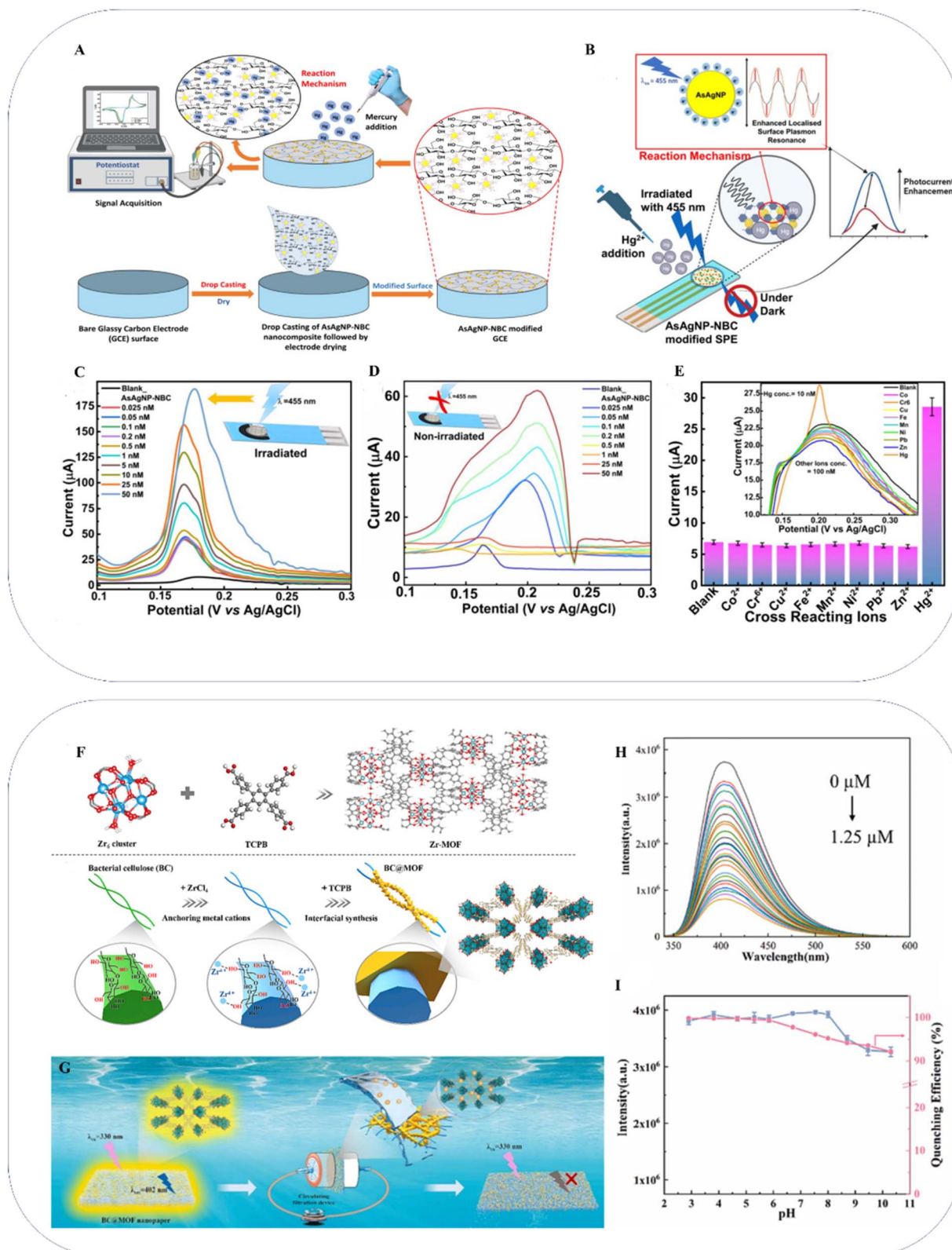
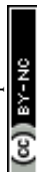
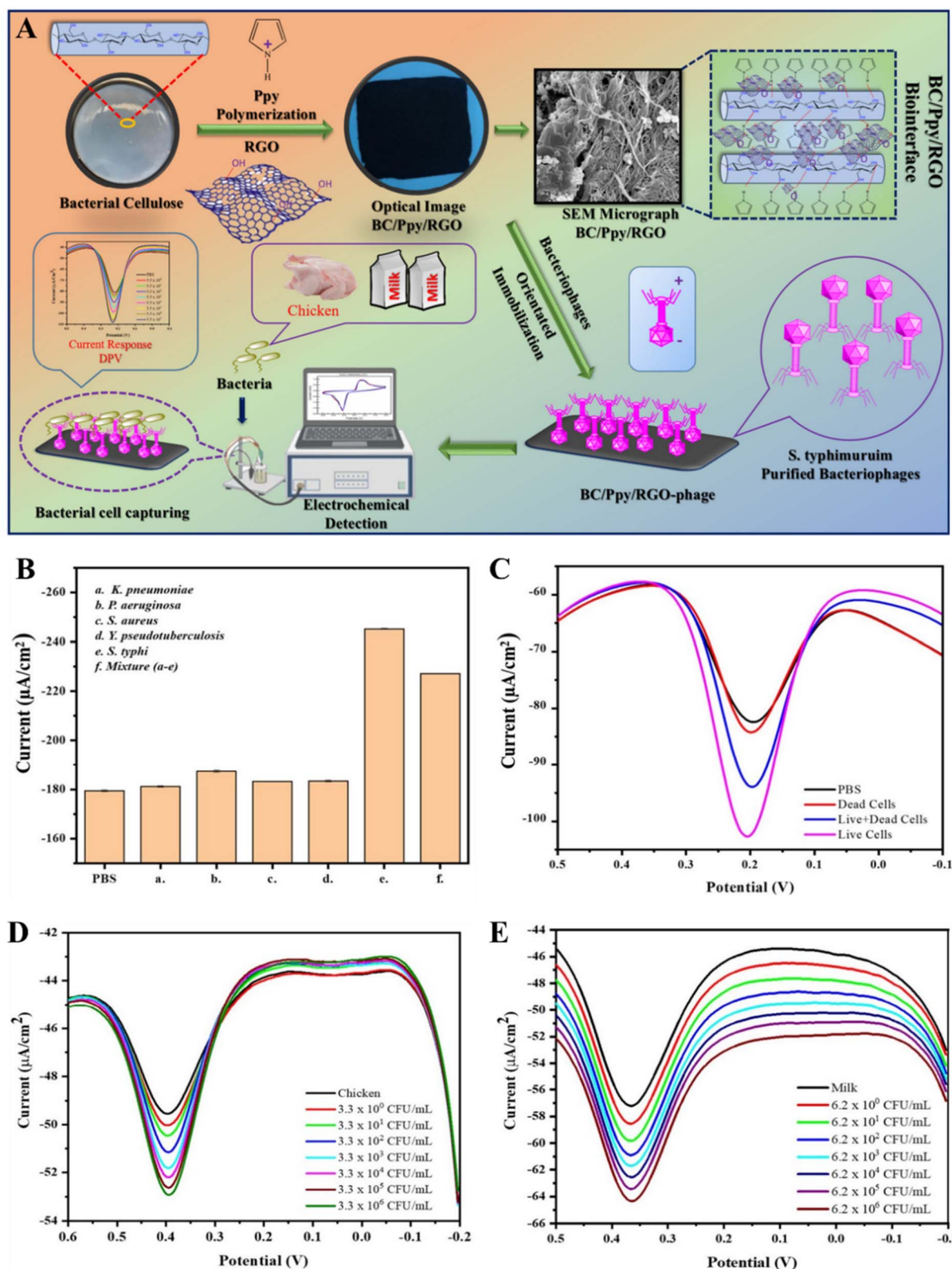
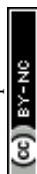


Fig. 7 BC-based biosensors for environmental monitoring. (A) Schematic of the 3-electrode system and electrode modification. (B) Schematic of the modified SPE and photocurrent enhancement experiment. (C and D) DPV measurements on an AsAgNP-NBC modified SPE chip with and without 455 nm irradiation (linear range: 25 pM–50 nM). (E) CV measurements for interfering ions (interfering metal ion concentration: 100 nM; Hg<sup>2+</sup> concentration: 10 nM). Reproduced with permission from ref. 123. Copyright (2024), Taylor & Francis. (F) Simplified conformations of Zr<sub>6</sub> clusters, TCPB linker, and network topologies, and *in situ* preparation of BC@Zr-MOF. (G) Schematic of Cr<sub>2</sub>O<sub>7</sub><sup>2-</sup> testing using PMs. (H) Emission spectra of BC@Zr-MOF (0.5 mg mL<sup>-1</sup>) dependent on concentration, at various Cr<sub>2</sub>O<sub>7</sub><sup>2-</sup> levels. (I) Quenching efficiency and stability of fluorescence across various pH values. Reproduced with permission from ref. 124. Copyright (2024), Elsevier B.V.





**Fig. 8** (A) Schematic illustrating fabrication of an electrochemical biosensor based on BC/Ppy/RGO functionalized with *S. typhimurium*-specific bacteriophage for detecting pathogens in milk and chicken. (B) Specificity analysis of the biosensor toward *S. typhimurium* against non-target bacteria. (C) Discrimination capability of the biosensor for live, dead, and mixed (live/dead) *S. typhimurium* cells. (D and E) Differential pulse voltammetry (DPV) response for *S. typhimurium* detection in (D) milk samples. (E) Chicken samples. Reproduced with permission from ref. 96, Copyright (2024), MDPI.



**3.2.3.1. Detection of foodborne pathogens.** Foodborne pathogens such as *Staphylococcus aureus*, *Escherichia coli*, and *Salmonella* spp. pose severe public health risks, necessitating rapid, on-site detection tools. Prompt identification of these pathogens is critical to preventing outbreaks and minimizing economic losses within the food industry. BC's 3D nanofibrillar network, characterized by its high porosity and interconnected pores, forms an open, hydrogel-like architecture. This unique structure significantly reduces the diffusion path length for analytes such as bacterial cells, proteins, or other biomolecules, allowing them to rapidly permeate the matrix and access immobilized biorecognition elements, including antibodies, bacteriophages, and aptamers. This facilitated transport kinetics, along with BC's functionalizable surface, results in biosensors with exceptional sensitivity, selectivity, and rapid response, ideal for pathogen detection.<sup>88,96,126,127</sup> In this regard, Hussain *et al.* successfully developed an ultrasensitive electrochemical biosensor for detecting *Salmonella typhimurium* by integrating a BC substrate modified with PPy and reduced graphene oxide (RGO), further functionalized with *S. typhimurium*-specific bacteriophages (Fig. 8A). This hybrid configuration produced a flexible, highly conductive platform that exploited the selective binding affinity of bacteriophages toward their bacterial hosts. The biosensor exhibited exceptional analytical performance, demonstrating high specificity, producing a distinct signal exclusively for *S. typhimurium* (Fig. 8B), and the ability to differentiate viable from non-viable cells, ensuring detection of only live pathogens (Fig. 8C). This system achieved ultra-sensitive detection in real food matrices, maintaining excellent sensitivity with detection limits of 3 CFU mL<sup>-1</sup> in chicken samples (Fig. 8D) and 5 CFU mL<sup>-1</sup> in milk (Fig. 8E).<sup>96</sup>

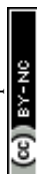
In another study, Ghasemi *et al.* developed a cost-effective conductometric nanobiosensor based on a BC/PPy/titanium dioxide-silver (BC/PPy/TiO<sub>2</sub>-Ag) nanocomposite film for the rapid detection of pathogenic bacteria in food samples. This biosensor operates on the principle of conductometry, where the binding of a target analyte induces a measurable change in the electrical conductivity (or resistance) of the nanocomposite film. BC provided a high-surface-area, porous scaffold that ensured efficient analyte transport, while PPy imparted excellent electrical conductivity and signal transduction capability. Meanwhile, TiO<sub>2</sub>-Ag NPs enhanced interfacial interactions, charge transfer, and bacterial capture efficiency. The sensors demonstrated preferential sensitivity toward Gram-negative over Gram-positive bacteria. The positively charged PPy and TiO<sub>2</sub>-Ag components interacted electrostatically with negatively charged bacterial cell walls, inducing measurable resistance variations that enabled real-time bacterial detection. The sensor's preferential sensitivity toward Gram-negative bacteria was governed by favorable electrostatic interactions with the positively charged nanocomposite, which induced measurable resistance changes for real-time monitoring.<sup>128</sup> Similarly, Farooq and colleagues designed an electrochemical biosensor by embedding bacteriophages within a surface-modified BC matrix. The incorporation of carboxylated multiwalled carbon nanotubes (c-MWCNTs) increased the available surface area for

phage immobilization, while polyethyleneimine (PEI) functionalization introduced positive surface charges, promoting oriented phage binding. This electrochemical biosensor, based on BC/phage, demonstrated effective discrimination of live *Staphylococcus aureus* cells within live/dead, exhibiting concomitant anti-staphylococcal activity. This ultra-sensitive biosensor achieved detection limits of 5 CFU mL<sup>-1</sup> and 3 CFU mL<sup>-1</sup> in milk and phosphate-buffered saline (PBS), respectively, within 30 minutes.<sup>129</sup>

**3.2.3.2. Detection of pesticide residues.** BC's characteristics make it suitable for fabricating flexible substrates that can directly collect contaminants through physical swabbing on curved food surfaces.<sup>130,131</sup> Ensuring food safety requires minimizing exposure to persistent agrochemicals such as organophosphates, carbamates, and dithiocarbamates, which remain on fruits, vegetables, and juices and are associated with endocrine disruption, neurotoxicity, and carcinogenicity. BC-based substrates demonstrate excellent analytical performance for detecting pesticide residues on food surfaces by leveraging their flexibility for direct swabbing of curved areas, ensuring efficient residue collection and superior analytical performance. While traditional methods such as gas chromatography-mass spectrometry (GC-MS) and high-performance liquid chromatography (HPLC) provide high accuracy, they are costly, time-consuming, and non-portable, which limits their suitability for on-site screening. BC-based biosensors effectively circumvent these limitations by integrating biological or physical transduction mechanisms into disposable, flexible platforms.<sup>90,130,131</sup>

A prominent application of BC is in SERS, where its nanofibrillar structure provides a high surface area for the efficient dispersion of plasmonic nanoparticles (*e.g.*, AuNPs, AgNPs), creating dense electromagnetic "hotspots" that significantly enhance Raman signals. For instance, a flexible BC/AuNPs nanocomposite SERS substrate was developed to detect thiram, a widely used dithiocarbamate fungicide. When tested on apple surfaces using "paste-and-peel" and "wiping" methods with a portable Raman spectrometer, the substrate achieved a detection limit of 0.98 ppm for thiram. The findings underscored the BC-based biosensor's analytical performance in terms of sensitivity, reproducibility, and stability, proving its suitability for rapid detection (within 8 minutes) and quantitative analysis of pesticides on food surfaces.<sup>131</sup> Similarly, Lospinoso *et al.* synthesized AuNPs@BC composites by *in situ* chemical reduction of Au<sup>3+</sup> ions, yielding a high-surface-area substrate with localized surface plasmon resonance (LSPR) hotspots and a bulk sensitivity of 72 nm RIU<sup>-1</sup>. This system achieved a detection limit of 0.24 ppm for thiram, meeting regulatory thresholds.<sup>90</sup>

In another study, a biodegradable and flexible SERS substrate was fabricated by compositing bacterial nanocellulose paper (BNCP) with AgNPs *via* a simple vacuum-filtration method (Fig. 9A). This process resulted in AgNPs being directly adhered to the 3D nanofibrous network of the BNCP (Fig. 9B), which provided excellent SERS activity and signal uniformity. The composite maintained favorable optical transparency (Fig. 9C), a property that was strategically leveraged to



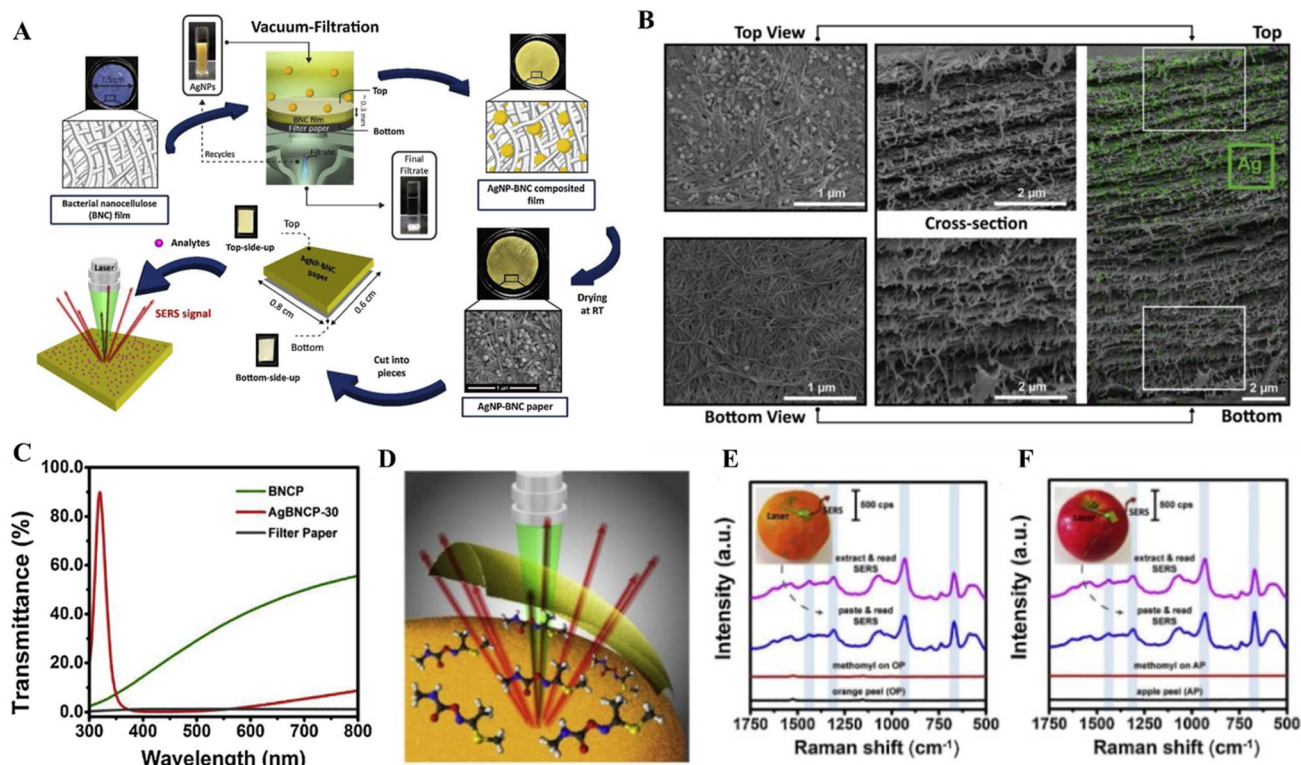


Fig. 9 (A) Schematic illustrating the fabrication of SERS-active AgNP-BNCPs. (B) SEM images of AgBNCP-30. (C) A comparison of the optical transmittance of filter paper, BNCP, and AgBNCP-30. (D) Schematic of the "paste-and-read" method for detecting methomyl by AgNP-BNCPs. (E and F) Raman and SERS spectra of methomyl on orange (E) and apple (F) peels, comparing "paste-and-read" (blue), "extract-and-read" (pink), and measurements without AgNP-BNCP (red); black lines represent the Raman spectra of the fruit peels without methomyl. Reproduced with permission from ref. 130. Copyright (2020), Elsevier Ltd.

develop a rapid, user-friendly "paste-and-read" SERS method (Fig. 9D). As shown in Fig. 9E and F, this method allowed direct detection of the carbamate pesticide methomyl on orange and apple peels without requiring complex extraction steps, achieving clear spectral differentiation from untreated samples.<sup>130</sup>

**3.2.3.3. Detection of heavy metal contamination.** Heavy metals such as copper ( $\text{Cu}^{2+}$ ), cadmium ( $\text{Cd}^{2+}$ ), lead ( $\text{Pb}^{2+}$ ), and mercury ( $\text{Hg}^{2+}$ ) can enter the food chain through agricultural runoff, industrial pollution, and food packaging, resulting in bioaccumulation and severe health risks, including oxidative stress, renal impairment, and developmental disorders. Monitoring these contaminants in foodstuffs and processing environments is critical for public health. To address this, BC-based biosensors offer a simple, cost-effective, and portable solution for screening heavy metal contamination in foodstuffs.<sup>118,132</sup> A notable example is a colorimetric sensor developed by Sheikh-zadeh *et al.*, where curcumin was embedded in BC nanofibers for  $\text{Pb}^{2+}$  detection in rice. The sensor exhibited a distinct color change from orange to red upon  $\text{Pb}^{2+}$  binding, achieving detection limits of 9  $\mu\text{M}$  (naked-eye observation) and 0.9  $\mu\text{M}$  (image processing), highlighting its potential for low-cost, on-site metal ion monitoring.<sup>133</sup>

More recently, Zhang *et al.* fabricated a portable fluorescent BC film (Y-CDs@BCM) by anchoring yellow-emitting carbon

dots (Y-CDs) onto the BC matrix for  $\text{Cu}^{2+}$  detection. The BC substrate prevented aggregation-induced quenching of the Y-CDs while providing mechanical stability and portability. Detection was based on the inner filter effect (IFE), where  $\text{Cu}^{2+}$  selectively quenched fluorescence with a detection limit of 7.76 nM, enabling rapid analysis in complex samples such as pig liver, human serum, and environmental water. Integration with smartphone-based colorimetric readout further enhanced its field applicability. The excellent biocompatibility of the Y-CDs, confirmed through cell viability assays and *in vivo* imaging in freshwater shrimp, highlights their suitability for biological applications,<sup>27</sup> further expanding the applications of BC-based biosensors in food safety.

**3.2.3.4. Intelligent packaging and spoilage monitoring.** Intelligent biosensor packaging is an efficient technology that can directly and accurately indicate food quality without complex operations, aiming to minimize food loss across the supply chain.<sup>134,135</sup> These systems translate complex biochemical changes associated with spoilage into simple, understandable signals, enabling real-time monitoring without complex operations. BC's excellent biocompatibility ensures safe interaction with food without compromising integrity or introducing contaminants, while simultaneously acting as both a structural support and an efficient diffusion medium, facilitating the rapid transport of volatile spoilage compounds to embedded



sensing elements. These films could detect both gamma radiation exposure and bacterial contamination.<sup>136</sup> BC-based biosensors enable real-time, non-destructive monitoring of food spoilage by capitalizing on pH fluctuations induced by microbial metabolites, specifically volatile amines. These fluctuations are quantitatively transduced into visible colorimetric or fluorescent signals using embedded indicators. Incorporating natural pigments, such as anthocyanins from red cabbage extract (RCE), preferred for their broad, visible color spectrum across pH ranges (red in acid to green/yellow in base) and their Generally Recognized as Safe (GRAS) status, offering a sustainable, eco-friendly alternative to synthetic dyes.<sup>137,138</sup>

RCE-infused BC films, typically prepared *via* ethanol–water maceration and cross-linked with agents such as glutaraldehyde for improved stability, yield edible films suitable for direct food contact. This technology has been successfully demonstrated in detecting spoilage in cucumbers, with the film's color change correlating to bacterial growth and pH increase.<sup>137</sup> pH sensors can be used to monitor the pH of various beverages. Immobilizing red cabbage anthocyanins (RSD) on a BC membrane yielded a novel edible pH sensor. This sensor exhibited a clear colorimetric response (red to purple, blue-gray, and yellow) across a pH range of 1–14, with linear response behavior between pH 1–6 and 8–12, and a rapid response time of 4

minutes with <1% variation, confirming its potential for intelligent food packaging systems. This pH sensor successfully distinguished spoiled milk from fresh milk, making it ideal for intelligent packaging systems.<sup>139</sup>

Starch-based pH-sensing films developed by Poljaček *et al.* exhibit a visible color change (red/pink to purple, blue, and green) across a pH range of 2.0 to 10.5. These films, incorporating BNC and red cabbage anthocyanins (RCA), demonstrate the potential for visual pH monitoring in smart packaging applications, with their colorimetric properties influenced by structural and intermolecular interactions. Additionally, the films' adhesion to commercially available packaging materials for raw meat was evaluated, indicating their feasibility for practical applications.<sup>140</sup> Furthering this research, another study developed an intelligent, pH-responsive film based on BC/gelatin/fluorescein isothiocyanate/PCA (BC/GA/FITC/PCA) for the visual monitoring of shrimp freshness (Fig. 10A). Upon exposure to ammonia, the film exhibited both colorimetric and fluorometric responses: under daylight, the film transitioned from purple to green with increasing ammonia concentration, while under UV illumination (254 nm and 365 nm), blue-green fluorescence increased, with a detection limit of 170 ppb (Fig. 10B). Control experiments with BC/GA films confirmed the contribution of FITC and PCA to the color and fluorescence

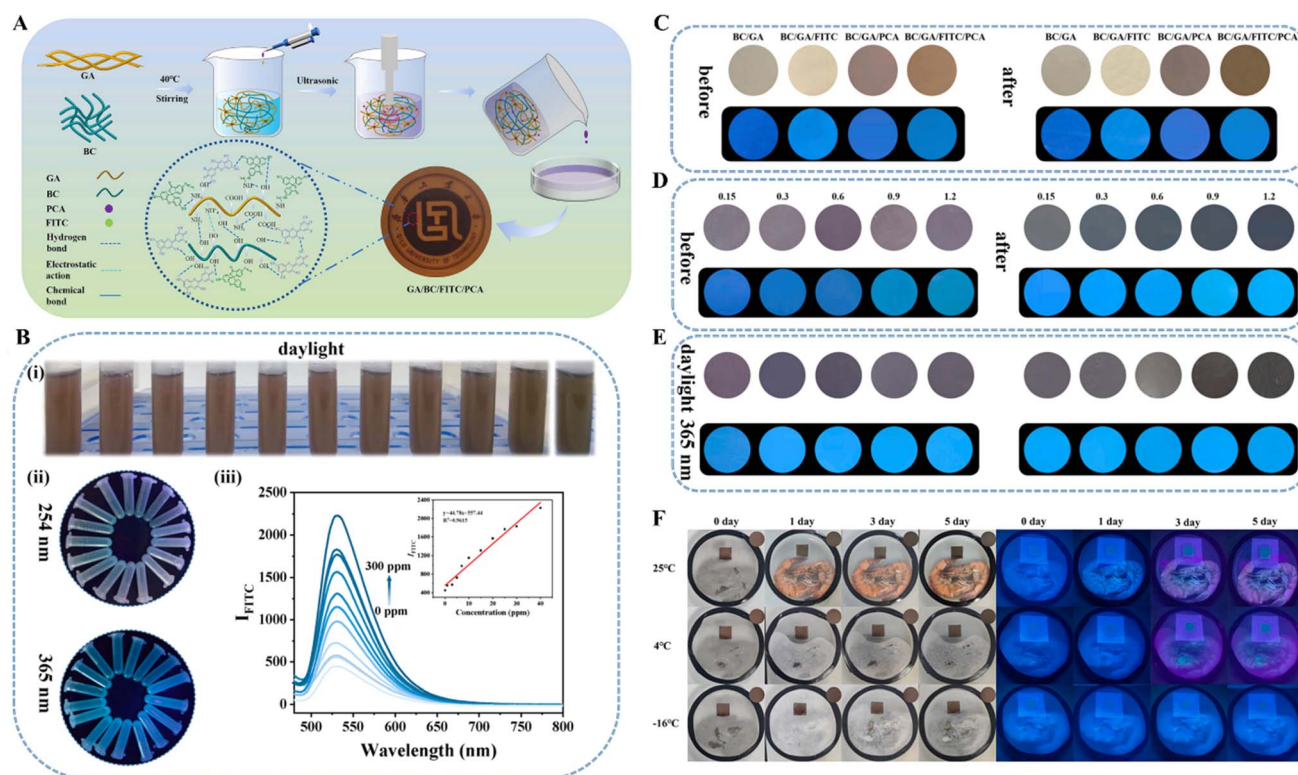


**Fig. 10** (A) Schematic representation of the fabrication process, structural components, and key interactions within the BC/GA/FITC/PCA film. (B) The colorimetric and fluorometric response of the BC/GA/FITC/PCA film to various ammonia concentrations (0–300 ppm) after a 5-minute reaction time: (i) images under daylight and UV illumination (254 nm and 365 nm); (ii) fluorescence intensity curves, and linear fits. (C) Colorimetric response of BC/GA films (before and after a 3-minute reaction with 3000 ppm ammonia) under daylight and 365 nm UV light. (D) Colorimetric response of BC/GA/FITC/PCA films containing varying concentrations of FITC. (E) Colorimetric response of BC/GA/FITC/PCA films at various reaction times. (F) Real-time monitoring of fresh shrimp freshness under various storage conditions. Reproduced with permission from ref. 141. Copyright (2024), Elsevier B.V.

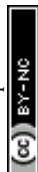


**Table 3** Overview of AI- and ML-assisted biosensor developments: key applications, findings, and associated challenges

Category	Key applications/findings	Challenges/limitations
AI and machine learning integration	AI techniques ( <i>e.g.</i> , support vector machines, decision trees, convolutional neural networks, recurrent neural networks) enhance signal discrimination, noise reduction, and multi-dimensional data analysis, improving sensitivity and specificity. <sup>102,160,161,165</sup> Data augmentation and synthetic data generation improve model robustness and predictive accuracy. <sup>161,163</sup>	Limited interpretability and explainability hinder clinical and regulatory acceptance. <sup>166–168</sup> Reliance on high-quality annotated datasets restricts generalizability. Computational demands limit real-time applications. <sup>168,169</sup> Integration is nascent, with few studies on end-to-end validation in complex biological matrices. <sup>170</sup>
Sensitivity and specificity enhancement	AI-driven biosensors achieve lower limits of detection and improved selectivity for pathogens, biomarkers, and toxins with high accuracy. <sup>102,160,162,171</sup>	Multi-analyte detection remains challenging due to signal overlap and batch effects. <sup>166,167</sup>
Data handling and augmentation	Techniques such as geometric transformations and variational autoencoders expand datasets and improve generalization. <sup>163,172</sup> Hybrid AI models combining imaging and electrochemical data enhance calibration and reliability. <sup>172</sup>	Synthetic data may introduce biases if not validated. <sup>163</sup> Lack of standardized preprocessing and augmentation protocols hinders reproducibility and cross-study comparison. <sup>168,173</sup>
Practical deployment and real-time applications	AI-enhanced biosensors enable portable, low-cost, real-time monitoring for point-of-care (POC) and wearable use. <sup>174</sup>	Regulatory compliance, data privacy, and ethics underexplored. <sup>167,174</sup> Transition to commercial products hindered by limited large-scale validation. <sup>164</sup> AI model complexity and data processing can increase costs and lengthen the development period. <sup>166</sup>

changes (Fig. 10C and D), and reaction time studies demonstrated rapid response kinetics (Fig. 10E). Importantly, real-time monitoring of shrimp freshness under different storage conditions revealed that the film's color changes correlated with the total volatile basic nitrogen (TVBN) value, validating its effectiveness as a simple and reliable tool for *in situ* freshness detection (Fig. 10F).<sup>141</sup>

### 3.3. Application of artificial intelligence (AI) in biosensor development

The integration of AI methodologies such as machine learning (ML) and deep learning into biosensor design and analysis has become a transformative approach in recent years. In particular, these technologies have enhanced detection accuracy, analytical efficiency, and data interpretability, marking a paradigm shift from conventional signal processing to intelligent biosensing systems.<sup>82,159,160</sup> Despite these advancements, challenges remain in translating AI-integrated biosensors from laboratory prototypes to commercial systems. Major barriers include the need for validated datasets, the limited interpretability of complex algorithms, and the computational cost.<sup>161–164</sup> Table 3 summarizes an overview of current progress in AI-enhanced biosensor development, highlighting key strengths, limitations, and emerging research directions.

## 4. Challenges and future perspective

The advancement of BC-based biosensors reflects a balance between the material's intrinsic advantages, such as biocompatibility, high porosity, and biodegradability, and the practical

challenges that hinder large-scale commercialization. As a microbial-derived nanofibrillar polymer, BC features a unique 3D reticular architecture that enables rapid analyte diffusion and efficient biomolecule immobilization, outperforming many synthetic and plant-based counterparts.<sup>175</sup> Furthermore, precise control over BC's structural and morphological properties allows the design of biosensors tailored for specific applications.<sup>66,176</sup> Despite the significant progress in BC-based biosensor development, challenges remain to its widespread adoption. The primary challenges lie in the scalability, cost, and complexity of BC production. Current fermentation processes are relatively slow, resource-intensive, and prone to batch-to-batch variability, which can compromise sensor reproducibility. Addressing these limitations requires optimizing production efficiency and scalability through metabolic and genetic engineering of cellulose-producing strains to enhance yield and control fibril architecture. Utilizing low-cost carbon sources, such as agro-industrial by-products or food waste, can further reduce production costs while promoting environmental sustainability.<sup>177</sup> In parallel, innovations in bioreactor design and continuous fermentation systems could enable more consistent and large-scale BC production suitable for commercial biosensing applications.<sup>66</sup> Co-culture strategies involving yeast or fungi, such as *Komagataeibacter-Saccharomyces* hybrids, have shown promise in improving yield through symbiotic metabolite exchange; however, challenges related to microbial stability and downstream separation remain to be addressed.<sup>178,179</sup>

Functionalization represents another critical challenge in advancing BC-based biosensors. Although the inherent



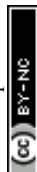
hydrophilicity of pristine BC supports the physical adsorption of biomolecules, it hinders the formation of stable covalent bonds with conductive or enzymatic components. Moreover, as an inherently non-conductive biopolymer, pristine BC exhibits restricted utility in electrochemical sensing platforms, necessitating its modification to achieve efficient electron transfer and signal amplification.<sup>180</sup> Incorporating conductive nanomaterials such as graphene,<sup>33</sup> MXenes,<sup>181</sup> metal NPs (e.g., Au, Ag),<sup>90,182</sup> and conducting polymers like PPy<sup>22</sup> could be an effective strategy to enhance BC's electrical performance. These nanostructures improve charge mobility and interfacial electron exchange, thereby significantly boosting sensor sensitivity and transduction efficiency. However, *ex situ* impregnation often results in weak interfacial bonding (e.g., hydrogen or van der Waals interactions), leading to NP aggregation, leaching in physiological environments, and inconsistencies in analytical performance.<sup>159</sup> In contrast, *in situ* biosynthesis offers a more sustainable and integrated approach, enabling the direct incorporation of nanomaterials during microbial fermentation.<sup>183</sup> Nonetheless, the addition of metal precursors or conductive agents can trigger cytotoxicity, impair cellulose synthase functionality, and form incomplete conductive networks.<sup>184</sup> Enzymatic modifications, such as laccase/TEMPO-mediated oxidation for carboxyl group introduction, offer enhanced specificity but are constrained by low reaction kinetics and restricted penetration into BC's crystalline structure.<sup>185</sup> For example, immobilized enzymes like glucose oxidase typically exhibit activity losses after multiple cycles due to diffusion constraints and conformational changes.<sup>186</sup> These limitations exacerbate performance inconsistencies, particularly in complex biological matrices where biofouling amplifies signal noise.<sup>187</sup>

The functionalization challenges are compounded by BC's sensitivity to environmental fluctuations in pH, temperature, and humidity, which can compromise structural integrity and biomolecule stability,<sup>83,141</sup> thereby affecting sensing accuracy. Such vulnerabilities restrict its detection range to specific analytes and often require chemical tailoring or hybridization with complementary materials to enable the detection of small molecules or ionic species.<sup>36,41</sup> To address these, future research avenues should focus on advanced hybridization strategies, integrating BC with nanostructured materials to improve electron transfer, enhance sensitivity, and expand its operational range. Surface engineering techniques, including plasma-assisted activation, covalent grafting, and bioorthogonal chemistry, offer promising avenues for achieving uniform, stable, and bioactive interfaces that maintain the functionality of immobilized biomolecules.<sup>188–190</sup> Additionally, hybrid composites incorporating photoactive or plasmonic nanostructures can expand BC's functionality beyond electrochemical detection, enabling the development of multimodal sensing platforms capable of optical, electrochemical, and piezoresistive transduction.<sup>40</sup>

Moving beyond simple surface modification, the field must now focus on developing reproducible, one-pot *in situ* strategies to engineer BC at the nanoscale, creating "smart" hybrids with built-in conductivity or recognition sites that eliminate complex

post-processing.<sup>66</sup> Advanced fabrication techniques such as 3D printing, electrospinning, and microfluidics offer new opportunities to design sophisticated, multifunctional biosensing architectures, paving the way for innovative biosensing solutions that leverage BC's inherent advantages.<sup>191,192</sup> These methods can facilitate miniaturization, high throughput, and rapid response capabilities for multiplexed diagnostics and wearable biosensors for non-invasive, continuous health monitoring.<sup>26</sup> The use of 3D printing technology offers an advanced and versatile approach to biosensor fabrication compared to conventional manufacturing methods.<sup>193</sup> In particular, the growing demand for wearable and POC biosensors, which provide non-invasive and user-friendly health monitoring, has highlighted the potential of 3D-printed biosensors. This technology allows for the creation of customizable biosensor architectures with controlled porosity, mechanical properties, and spatial arrangements of sensing elements, enabling the design of devices tailored to specific applications.<sup>193–195</sup> Despite these advantages, several challenges limit the full exploitation of BC in 3D-printed biosensors. Maintaining bacterial viability during the fabrication of living BC-based materials with complex geometries remains a major obstacle, especially for constructs designed to regenerate their cellulose networks after damage.<sup>196</sup> Furthermore, variations in printing parameters, the lack of well-defined material standards, and the absence of standardized protocols to ensure both safety and functional effectiveness in 3D printing underscore a critical knowledge gap for 3D-printed biosensors.<sup>193,197</sup>

Integration of BC into flexible, wearable, and implantable biosensing devices represents another promising frontier. The natural conformability, breathability, and biocompatibility of BC make it an excellent candidate for skin-mounted or tissue-interfacing sensors capable of continuous, real-time physiological monitoring. However, achieving stable signal transmission under mechanical deformation remains challenging. Reinforcing BC with elastomeric polymers or encapsulating it within soft matrices such as Ecoflex can significantly improve stretchability and mechanical resilience while preserving biocompatibility.<sup>113</sup> These next-generation BC composites could revolutionize personalized healthcare by enabling non-invasive tracking of vital biomarkers such as glucose, lactate, and inflammatory cytokines. Beyond healthcare, BC-based biosensors hold significant promise for smart and intelligent food packaging as well as environmental monitoring. When combined with natural colorimetric agents, enzymatic probes, or fluorescent dyes, BC can be used to fabricate intelligent films that visually signal spoilage, microbial contamination, or chemical hazards. Such developments not only enhance food safety but also align with global sustainability goals by minimizing waste and improving resource management. Coupling these responsive films with smartphone-based imaging or wireless readout interfaces will enable real-time, user-friendly monitoring throughout the food supply chain. Such innovations not only enhance food safety but also contribute to global sustainability by reducing waste and optimizing resource management.



As biosensing systems evolve, the integration of BC-based devices with digital technologies such as AI, the Internet of Things (IoT), and big data analytics will be transformative.<sup>198,199</sup> Embedding BC biosensors within connected platforms can enable automated data acquisition and real-time analysis. AI-driven algorithms could interpret complex biosensor data patterns to provide personalized health insights or early warnings of environmental hazards. By bridging fundamental materials research with practical engineering applications, BC can evolve from a promising biopolymer into a multifunctional platform for next-generation. Such systems can be poised to transition from simple detection tools to intelligent, self-learning diagnostic technologies that support the future of precision health and environmental monitoring. To achieve this transformation, however, key regulatory and commercialization challenges must be addressed. Establishing standardized production protocols, ensuring biocompatibility and long-term stability, and implementing rigorous quality control frameworks are critical for enabling industrial-scale manufacturing. Moreover, close collaboration among materials scientists, engineers, clinicians, and policymakers will be vital to overcoming these barriers, accelerating technology translation, and realizing the full potential of BC-based biosensors in real-world applications.

## 5. Conclusion

The sustainable, nanostructured nature of BC positions it as a platform for a new era of biosensors, creating integrated and resilient technologies that bridge biological design and analytical precision. Its unique nanofibrillar architecture, coupled with excellent biocompatibility and tunable physicochemical properties, makes BC a superior alternative to conventional polymeric substrates. The interconnected, porous 3D network offers an extensive surface area that supports the high-density immobilization of enzymes, antibodies, and other biorecognition molecules. This structural advantage enables the engineering of robust, sensitive, and selective biosensors optimized for the precise detection of target analytes. Moreover, the tunable morphology, chemical modifiability, and mechanical flexibility of BC enable the fabrication of versatile sensing systems tailored to diverse diagnostic and analytical applications. These attributes not only enhance sensor performance but also promote the development of minimally invasive, wearable, and implantable devices, while aligning with the principles of green chemistry and global efforts toward renewable, eco-friendly technologies. This review highlights the diverse applications of BC-based biosensors across critical domains, including high-sensitivity diagnostics for early disease detection, environmental monitoring, and food safety assessment. By outlining the current landscape of BC-based biosensors, including fabrication strategies, surface functionalization techniques, and performance benchmarks, it highlights their transformative potential while candidly addressing persistent challenges, such as scalability limitations in microbial production, batch-to-batch variability, and sensitivity to environmental factors like humidity or pH. Future prospects

hinge on interdisciplinary innovations, including advanced bioprocess engineering for cost-effective synthesis, hybrid nanocomposites for enhanced signal transduction, and integration with digital interfaces for AI-driven data analytics, thereby propelling ongoing advancements in sustainable biosensor technology toward broader commercialization and societal impact.

## Conflicts of interest

The authors have no competing interests to declare that are relevant to the content of this article.

## Abbreviations

AsAgNPs	Ascorbic acid-capped silver nanoparticles
APT	Attapulgit
BC	Bacterial cellulose
BCM	Bacterial cellulose membrane
BCNF	Bacterial cellulose nanofibers
BNCP	Bacterial nanocellulose paper
BOD	Biochemical oxygen demand
Cd <sup>2+</sup>	Cadmium
CdTe	Cadmium telluride quantum dots
c-MWCNTs	Carboxylated multiwalled carbon nanotubes
CMC	Carboxymethyl cellulose
CV	Cyclic voltammetry
ECM	Extracellular matrix
FeO	Ferrous oxide
FITC	Fluorescein isothiocyanate
GCE	Glassy carbon electrode
GA	Gelatin
Gox	Glucose oxidase
GSH	Glutathione
Au	Gold
GG	Guar gum
GO	Graphene oxide
HB	Hemoglobin
HCI	Human-computer interaction
HRP	Horseradish peroxidase
KB	Ketjen black
Lac	Laccase
Pb <sup>2+</sup>	Lead
LOD	Limit of detection
MOFs	Metal-organic frameworks
Mb	Myoglobin
NBC	Nanocrystalline bacterial cellulose
NPs	Nanoparticles
NP/OP	Nasopharyngeal/oropharyngeal
NSCs	Neural stem cells
N-CDs	Nitrogen-doped carbon dots
OxBC	Oxidized bacterial cellulose
Pd	Palladium
HMP	Pentose phosphate
Pt	Platinum
POC	Point-of-care
PAni	Polyaniline
PEI	Polyethyleneimine



PPY	Polypyrrole
PVA	Polyvinyl alcohol
PVAN	Polyvinylaniline
PEDOT:PSS	Poly(3,4-ethylenedioxythiophene) polystyrene sulfonate
QDs	Quantum dots
QCM	Quartz crystal microbalance
QCS	Quaternized chitosan
PCA	Red cabbage
RCA	Red cabbage anthocyanins
RCE	Red cabbage extract
RSD	Relative standard deviation
SPE	Screen-printed electrode
SPCEs	Screen-printed carbon electrodes
SPAN	Self-doped polyaniline nanofibers
AgNPs	Silver nanoparticles
SERS	Surface-enhanced Raman scattering
ATRP	Surface-initiated atom transfer radical polymerization
TiO <sub>2</sub>	Titanium dioxide
TVBN	Total volatile basic nitrogen
TNF- $\alpha$	Tumor necrosis factor- $\alpha$
TCA	Tricarboxylic acid
ZIF-8	Zeolitic imidazolate framework-8
ZnO	Zinc oxide

## Data availability

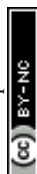
Data sharing is not applicable to this article as no new data were created or analyzed in this study.

## Acknowledgements

Funding from Agencia Estatal de Investigación (Ayuda RYC2023-042668-I financiada por MICIU/AEI/10.13039/501100011033 y por el FSE+). Artificial intelligence was used to assist in improving the language, clarity, and grammar of this manuscript.

## References

- 1 A. P. Garg and M. D. Joshi, in *Functionalized Nanomaterials for Biosensing and Bioelectronics Applications*, Elsevier, 2024, pp. 3–30.
- 2 S. C. de Assis, D. L. Morgado, D. T. Scheidt, S. S. de Souza, M. R. Cavallari, O. H. Ando Junior and E. Carrilho, *Biosensors*, 2023, **13**, 142.
- 3 M. Popescu and C. Ungureanu, *Coatings*, 2023, **13**, 486.
- 4 P. Lv, H. Zhou, A. Mensah, Q. Feng, D. Wang, X. Hu, Y. Cai, L. A. Lucia, D. Li and Q. Wei, *Chem. Eng. J.*, 2018, **351**, 177–188.
- 5 A. Williams, M. R. Aguilar, K. G. G. Pattiya Arachchillage, S. Chandra, S. Rangan, S. Ghosal Gupta and J. M. Artes Vivancos, *ACS Sustain. Chem. Eng.*, 2024, **12**, 10296–10312.
- 6 Y. Zhao, K. Q. Jin, J. D. Li, K. K. Sheng, W. H. Huang and Y. L. Liu, *Adv. Mater.*, 2023, e2305917, DOI: [10.1002/adma.202305917](https://doi.org/10.1002/adma.202305917).
- 7 G. Liu, Z. Lv, S. Batool, M. Z. Li, P. Zhao, L. Guo, Y. Wang, Y. Zhou and S. T. Han, *Small*, 2023, **19**, e2207879.
- 8 A. Yu, M. Zhu, C. Chen, Y. Li, H. Cui, S. Liu and Q. Zhao, *Adv. Healthcare Mater.*, 2024, **13**, e2302460.
- 9 M. H. Fakhr, I. L. Carrasco, D. Belyaev, J. Kang, Y. Shin, J.-S. Yeo, W.-G. Koh, J. Ham, A. Michaelis and J. Opitz, *Biosens. Bioelectron.*, 2024, **19**, 100503.
- 10 C. Ye and C.-T. Lin, *Microchim. Acta*, 2023, **190**, 183.
- 11 S. R. Benjamin, F. de Lima, V. A. d. Nascimento, G. M. de Andrade and R. B. Oriá, *Biosensors*, 2023, **13**, 689.
- 12 Q. Wang and Y. Feng, *Sens. Rev.*, 2025, **45**, 563–578.
- 13 D. Yang, T. Zhang, T. Jia, K. Yang, T. Lian and H. Wang, *Sens. Actuators, B*, 2025, **424**, 136917.
- 14 P. R. Mariappan, N. R. Barveen, C.-C. Chiu, C.-Y. Kuo and Y.-W. Cheng, *Surf. Interfaces*, 2025, **64**, 106473.
- 15 E. A. Kamoun, M. Elsbahy, A. M. Mohamed Elbadry, E. B. Abdelazim, A. A. Mohsen, M. A. Aleem, H. Gao, N. G. Eissa, I. Elghamry and S. A. Salim, *ACS Omega*, 2025, **10**, 8816–8831.
- 16 F. Ciftci, A. Koyuncu and M. Ghorbanpour, *Cellulose*, 2025, 1–31.
- 17 M. Lv, L. Wang, Y. Hou, X. Qiao and X. Luo, *Anal. Chim. Acta*, 2025, **1339**, 343610.
- 18 Y. Xu, Q. Luo, L. Yang, S. Zhang, Y. Huang, Y. Sun, W. Wei, M. Xie and Y. Hu, *Microchem. J.*, 2025, 114528.
- 19 Q. Xiang, H. Zhang, Z. Liu, Y. Zhao and H. Tan, *Chem. Eng. J.*, 2024, **480**, 147825.
- 20 Y. Hashempour, F. Mortezaadeh, S. Rezaei, M. Salehipour, F. Gholami-Borujeni, P. Ebrahimnejad and M. Mogharabi-Manzari, *Int. J. Biol. Macromol.*, 2025, **292**, 139288.
- 21 O. Ziyilan, H. H. Ipekci, S. Unal, M. Erkartal, U. Sen and A. Uzunoglu, *Mater. Sci. Eng., B*, 2025, **314**, 118045.
- 22 Z. Yuan, H. Yin, M. Zheng, X. Chen, W. Peng, H. Zhou, J. Xing, L. Wang and S. Hu, *Carbohydr. Polym.*, 2025, **349**, 122963.
- 23 M. Xiao, X. Dong, Z. Wang, L. Zhang, Z. Lu and B. Du, *J. Alloys Compd.*, 2025, 181239.
- 24 P. K. Drishya, M. V. Reddy, G. Mohanakrishna, O. Sarkar, Isha, M. V. Rohit, A. Patel and Y.-C. Chang, *Macromol.*, 2025, **5**, 21.
- 25 M. Lv, Y. Li, X. Qiao, X. Zeng and X. Luo, *Anal. Chim. Acta*, 2024, **1316**, 342821.
- 26 N. O. Gomes, E. Carrilho, S. A. S. Machado and L. F. Sgobbi, *Electrochim. Acta*, 2020, **349**, 136341.
- 27 H. Zhang, Q. Zhang, X. Ji, B. Han, J. Wang and C. Han, *Molecules*, 2025, **30**, 3633.
- 28 X. Zhang, J. Yao, Y. Yan, Y. Zhang, Y. Tang and Y. Yang, *ACS Appl. Mater. Interfaces*, 2024, **16**, 60902–60911.
- 29 X. Wang, T. Sun, H. Yang, J. Zhang, L. Wang, Y. Zhang and N. Zhou, *Food Control*, 2025, **175**, 111300.
- 30 N. Sriplai, R. Mangayil, A. Pammo, V. Santala, S. Tuukkanen and S. Pinitsoontorn, *Carbohydr. Polym.*, 2020, **231**, 115730.
- 31 F. Jabbari and V. Babaeipour, *Int. J. Polym. Mater. Polym. Biomater.*, 2024, **73**, 455–477.
- 32 B. Dong, D. Yu, P. Lu, Z. Song, W. Chen, F. Zhang, B. Li, H. Wang and W. Liu, *Carbohydr. Polym.*, 2024, **326**, 121621.



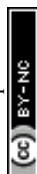
- 33 C. Wang, R. Wu, L. Wang and X. Wang, *Chem. Eng. J.*, 2024, **481**, 148390.
- 34 J. P. Ramoso, M. Rasekh and W. Balachandran, *Biosensors*, 2025, **15**, 586.
- 35 A. Kumar and P. Maiti, *Mater. Adv.*, 2024, **5**, 3563–3586.
- 36 S. Kamel and T. A. Khattab, *Biosensors*, 2020, **10**, 67.
- 37 K. Spychalska, D. Zajac, S. Baluta, K. Halicka and J. Cabaj, *Polymers*, 2020, **12**, 1154.
- 38 P. Boonkrong, N. Promphet, N. Rodthongkum and P. Puthongkham, *Microchem. J.*, 2025, **210**, 112951.
- 39 M. Shayan, M. S. Koo, R. Abouzeid, Y. Chen, J. Gwon and Q. Wu, *Cellulose*, 2025, 1–14.
- 40 S. C. de Assis, D. L. Morgado, D. T. Scheidt, S. S. de Souza, M. R. Cavallari, O. H. Ando Junior and E. Carrilho, *Biosensors*, 2023, **13**, 142.
- 41 F. G. Torres, O. P. Troncoso, K. N. Gonzales, R. M. Sari and S. Gea, *Med. Devices Sens.*, 2020, **3**, e10102.
- 42 G. Bayramoglu, S. Tilki and M. Y. Arica, *Cellulose*, 2024, **31**, 5133–5149.
- 43 T. Yi, H. Zhao, Q. Mo, D. Pan, Y. Liu, L. Huang, H. Xu, B. Hu and H. Song, *Materials*, 2020, **13**, 5062.
- 44 S. Mishra, P. K. Singh, R. Pattnaik, S. Kumar, S. K. Ojha, H. Srichandan, P. K. Parhi, R. K. Jyothi and P. K. Sarangi, *Front. Bioeng. Biotechnol.*, 2022, **10**, 780409.
- 45 P. Grzybek, G. Dudek and B. van der Bruggen, *Chem. Eng. J.*, 2024, 153500.
- 46 A. K. Saleh, J. B. Ray, M. H. El-Sayed, A. I. Alalawy, N. Omer, M. A. Abdelaziz and R. Abouzeid, *Int. J. Biol. Macromol.*, 2024, **264**, 130454.
- 47 F. G. Torres, J. J. Arroyo and O. P. Troncoso, *Mater. Sci. Eng., C*, 2019, **98**, 1277–1293.
- 48 H. Khan, A. Kadam and D. Dutt, *Carbohydr. Polym.*, 2020, **229**, 115513.
- 49 D. Núñez, P. Oyarzún, R. Cáceres, E. Elgueta and M. Gamboa, *Front. Bioeng. Biotechnol.*, 2024, **12**, 1375984.
- 50 A. Pandit and R. Kumar, *J. Polym. Environ.*, 2021, **29**, 2738–2755.
- 51 M. Oprea, D. M. Panaitescu, C. A. Nicolae, A. R. Gabor, A. N. Frone, V. Raditoiu, R. Trusca and A. Casarica, *Polym. Degrad. Stabil.*, 2020, **179**, 109203.
- 52 A. Karlstaedt, R. Khanna, M. Thangam and H. Taegtmeier, *Circ. Res.*, 2020, **126**, 60–74.
- 53 M. Liu, L. Liu, S. Jia, S. Li, Y. Zou and C. Zhong, *Sci. Rep.*, 2018, **8**, 6266.
- 54 J. K. Muiruri, J. C. C. Yeo, Q. Zhu, E. Ye, X. J. Loh and Z. Li, *Eur. Polym. J.*, 2023, 112446.
- 55 S. Manan, M. W. Ullah, M. Ul-Islam, Z. Shi, M. Gauthier and G. Yang, *Prog. Mater. Sci.*, 2022, **129**, 100972.
- 56 V. D. Girard, J. Chaussé and P. Vermette, *J. Appl. Polym. Sci.*, 2024, **141**, e55163.
- 57 A. Singh, K. T. Walker, R. Ledesma-Amaro and T. Ellis, *Int. J. Mol. Sci.*, 2020, **21**, 9185.
- 58 B. S. Inoue, S. Streit, A. L. dos Santos Schneider and M. M. Meier, *Int. J. Biol. Macromol.*, 2020, **148**, 1098–1108.
- 59 W. Zhang, X.-c. Wang, X.-y. Li and F. Jiang, *Carbohydr. Polym.*, 2020, **236**, 116043.
- 60 A. Farahmand Kateshali, F. Moghzi, J. Soleimannejad and J. Janczak, *Inorg. Chem.*, 2024, **63**, 3560–3571.
- 61 S. Meng, Y. Zhang, N. Wu, C. Peng, Z. Huang, Z. Lin, C. Qi, Z. Liu and T. Kong, *Nano Res.*, 2023, **16**, 4067–4076.
- 62 S. Fooladi, M. H. Nematollahi, N. Rabiee and S. Irvani, *ACS Biomater. Sci. Eng.*, 2023, **9**, 2949–2969.
- 63 C. H. Sung, T. Hao, H. Fang, A. T. Nguyen, V. Perricone, H. Yu, W. Huang, E. Sarmiento, A. F. D. Ornelas and D. Lublin, *Adv. Mater.*, 2025, e09281.
- 64 M. P. Illa, K. Peddapapannagari, S. C. Raghavan, M. Khandelwal and C. S. Sharma, *Cellulose*, 2021, **28**, 10077–10097.
- 65 A. J. Akki, P. Jain, R. Kulkarni, R. V. Kulkarni, F. Zameer, V. R. Anjanapura and T. M. Aminabhavi, *Sens. Int.*, 2024, 100277.
- 66 M. Cabo Jr, F. Ebrahimi, J. R. Alston, R. Kulkarni, S. Kattel, K. Dellinger and D. Lajeunesse, *ACS Polym. Au*, 2025, DOI: [10.1021/acspolymersau.5c00074](https://doi.org/10.1021/acspolymersau.5c00074).
- 67 W. X. Cai, S. Q. Zhang, X. Wang, D. X. Wei and Z. Chen, *J. Polym. Sci.*, 2025, 1–21.
- 68 Z. Bai, W. Zeng, J. Deng, S. Zhou, C. Yang, T. Jin and H. Wei, *Sens. Actuators, A*, 2024, 115714.
- 69 L. Feng, X. Cao, Z. L. Wang and L. Zhang, *Nano Energy*, 2024, **120**, 109068.
- 70 C. Gao, Y. Liu, Z. Gu, J. Li, Y. Sun, W. Li, K. Liu, D. Xu, B. Yu and W. Xu, *Adv. Fiber Mater.*, 2024, 1–15.
- 71 S. Torgbo and P. Sukyai, *Polym. Degrad. Stab.*, 2020, **179**, 109232.
- 72 I. Sayah, C. Gervasi, S. Achour and T. Gervasi, *Fermentation*, 2024, **10**, 100.
- 73 R. E. Jabbour, J. S. Kang and H. F. Sobhi, *ACS Omega*, 2024, **9**, 20003–20011.
- 74 V. Naresh and N. Lee, *Sensors*, 2021, **21**, 1109.
- 75 K. Jin, C. Jin and Y. Wu, *Carbohydr. Polym.*, 2022, **283**, 119171.
- 76 A. Pandey, M. K. Singh and A. Singh, *J. Mater. Res.*, 2024, **39**, 2–18.
- 77 Y. Gai, L. Yang, W. Shen, F. Tan, Q. Yu, L. Zhang and D. Sun, *J. Mater. Chem. C*, 2024, **12**, 1763–1772.
- 78 E. Vasili, B. Azimi, M. P. Raut, D. A. Gregory, A. Mele, B. Liu, K. Römhild, M. Krieg, F. Claeysens and P. Cinelli, *Polymers*, 2025, **17**, 1162.
- 79 S. Dermol, B. Borin, D. Gregor-Sveteć, L. Slemenik Perse and G. Lavric, *Polymers*, 2024, **16**, 1527.
- 80 M. Adampourezare, B. Nikzad, S. Nasrollahzadeh, K. Asadpour-Zeynali, M. de la Guardia, J. E. N. Dolatabadi, F. Zhang and S. M. Jafari, *Microchem. J.*, 2024, 110944.
- 81 Y.-C. Huang, D. Khumsupan, S.-P. Lin, S. P. Santoso, H.-Y. Hsu and K.-C. Cheng, *Int. J. Biol. Macromol.*, 2024, **258**, 128977.
- 82 M. Sheraz, X.-F. Sun, A. Siddiqui, Y. Wang, S. Hu and R. Sun, *Sensors*, 2025, **25**, 645.
- 83 A. N. Shishparenok, V. V. Furman, N. V. Dobryakova and D. D. Zhdanov, *Polymers*, 2024, **16**, 2468.
- 84 H. K. Choi and J. Yoon, *Biosensors*, 2023, **13**, 492.



- 85 K. Quan, Y. Zeng, W. Zhang, F. Li, M. Li, Z. Qing and L. Wu, *Anal. Chim. Acta*, 2024, **1285**, 342008.
- 86 M.-J. Lee, J.-H. Shin, S.-H. Jung and B.-K. Oh, *Biosensors*, 2024, **15**, 2.
- 87 L. F. de Lima, A. L. Ferreira, I. Ranjan, R. G. Collman, W. R. de Araujo and C. de La Fuente-Nunez, *Cell Rep. Phys. Sci.*, 2023, **4**(8), 101476.
- 88 U. Farooq, M. W. Ullah, Q. Yang, A. Aziz, J. Xu, L. Zhou and S. Wang, *Biosens. Bioelectron.*, 2020, **157**, 112163.
- 89 H. Tomaşoğlu, E. Gumus, E. Zor and H. Bingol, *J. Pharm. Biomed. Anal.*, 2025, **5**, 100065.
- 90 D. Lospinoso, A. Colombelli, S. Pal, P. Creti, M. C. Martucci, G. Giancane, A. Licciulli, R. Rella and M. G. Manera, *Biosensors*, 2025, **15**, 69.
- 91 Z. Yuan, K. Chen, L. Dong, H. Zhou, Q. Liu, M. Jin, S. Zeng, X. Chen, J. Xing and G. Yang, *Chem. Eng. J.*, 2025, **509**, 161034.
- 92 M. Xiao, X. Dong, Z. Wang, X. Zhang, C. Yang, N. Jiang and B. Du, *Mater. Today Commun.*, 2025, **45**, 112459.
- 93 J. Huang, M. Zhao, Y. Hao and Q. Wei, *Adv. Mater. Technol.*, 2022, **7**, 2100617.
- 94 S. Tao, Q. Yang, J. Su, N. Zhang, L. Xu, H. Pan, T. Zhou, H. Zhang, K. Jin and J. Wang, *Colloids Surf., A*, 2025, 137447.
- 95 L. Wu, F. Wang, R. Qi, M. Li, J. Zhang, Y. Wu and W. Ye, *Polym. Compos.*, 2025, 1–11.
- 96 W. Hussain, H. Wang, X. Yang, M. W. Ullah, J. Hussain, N. Ullah, M. Ul-Islam, M. F. Awad and S. Wang, *Biosensors*, 2024, **14**, 500.
- 97 A. F. Kateshali, F. Moghzi, J. Soleimannejad and J. Janczak, *Sci. Rep.*, 2025, **15**, 16216.
- 98 L. F. de Lima, A. L. Ferreira, L. E. Dos Santos, K. L. P. Coelho, K. T. Santos, A. Schmidt, M. B. de Jesus, T. R. Paixão and W. R. de Araujo, *ACS Appl. Bio Mater.*, 2025, **8**(7), 6339–6349.
- 99 T. Siripongpreda, B. Somchob, N. Rodthongkum and V. P. Hoven, *Carbohydr. Polym.*, 2021, **256**, 117506.
- 100 J. Chen, J. Yang, Y. Lu, Z. Dai and H. Li, *Sens. Actuators, B*, 2026, **448**, 138929.
- 101 Y. Wu, Q. Nie, X. Zeng, P. Wei, C. Zhu, R. You, C. Lin and L. Lin, *Microchem. J.*, 2024, **200**, 110378.
- 102 T. J. Bondancia, A. C. Soares, M. Popolin-Neto, N. O. Gomes, P. A. Raymundo-Pereira, H. S. Barud, S. A. Machado, S. J. Ribeiro, M. E. Melendez and A. L. Carvalho, *Biomater. Adv.*, 2022, **134**, 112676.
- 103 J. Li, D. Lu, J. Yang, R. You, J. Chen, J. Weng and Y. Lu, *Cellulose*, 2023, **30**, 5187–5200.
- 104 M. Jose, M. T. Vijjapu, L. Neumaier, L. Rauter, A. H. Chakkunny, D. Corzo, R. Thoelen, A. Picard, J. Kosel and W. Deferme, *npj Flexible Electron.*, 2025, **9**, 46.
- 105 S. N. Ilhan, B. A. Yilmaz and F. Ciftci, *BME Front.*, 2025, **6**, 0109.
- 106 H. Melnyk, O. Havryliuk, I. Zaets, T. Sergeyeva, G. Zubova, V. Korovina, M. Scherbyna, L. Savinska, L. Khirunenko and E. Amler, *Polymers*, 2025, **17**, 2116.
- 107 M. Yang and K.-I. Choy, *Mater. Lett.*, 2021, **288**, 129335.
- 108 O. Eskilson, E. Zattarin, L. Berglund, K. Oksman, K. Hanna, J. Rakar, P. Sivilér, M. Skog, I. Rinklake and R. Shamasha, *Mater. Today Bio*, 2023, **19**, 100574.
- 109 J. D. P. de Amorim, C. J. G. da Silva Junior, A. D. L. M. de Medeiros, H. A. do Nascimento, M. Sarubbo, T. P. M. de Medeiros, A. F. d. S. Costa and L. A. Sarubbo, *Molecules*, 2022, **27**, 5580.
- 110 S. Zhang, F. Ding, Y. Liu and X. Ren, *Carbohydr. Polym.*, 2022, **292**, 119615.
- 111 O. Eskilson, S. B. Lindström, B. Sepulveda, M. M. Shahjamali, P. Güell-Grau, P. Sivilér, M. Skog, C. Aronsson, E. M. Björk and N. Nyberg, *Adv. Funct. Mater.*, 2020, **30**, 2004766.
- 112 R. R. Silva, P. A. Raymundo-Pereira, A. M. Campos, D. Wilson, C. G. Otoni, H. S. Barud, C. A. Costa, R. R. Domenegueti, D. T. Balogh and S. J. Ribeiro, *Talanta*, 2020, **218**, 121153.
- 113 C. Gao, Y. Liu, F. Gu, Z. Chen, Z. Su, H. Du, D. Xu, K. Liu and W. Xu, *Chem. Eng. J.*, 2023, **460**, 141769.
- 114 H. Zhi, X. Zhang, F. Wang, P. Wan and L. Feng, *ACS Appl. Mater. Interfaces*, 2021, **13**, 45987–45994.
- 115 M. Mahdavi, H. Emadi and S. R. Nabavi, *Nanoscale Adv.*, 2023, **5**, 4782–4797.
- 116 J. Yao, P. Ji, B. Wang, H. Wang and S. Chen, *Sens. Actuators, B*, 2018, **254**, 110–119.
- 117 P. Deshpande, S. Wankar, S. Mahajan, Y. Patil, J. Rajwade and A. Kulkarni, *J. Nat. Fibers*, 2023, **20**, 2218623.
- 118 P. Parizadeh, F. Moeinpour and F. S. Mohseni-Shahri, *Chemosphere*, 2023, **326**, 138459.
- 119 S. Song, Z. Liu, J. Zhang, C. Jiao, L. Ding and S. Yang, *Materials*, 2020, **13**, 3703.
- 120 X. Zhao, M. Yang, Y. Shi, L. Sun, H. Zheng, G. Gao, T. Ma and G. Li, *J. Hazard. Mater.*, 2024, 135267.
- 121 H. Asiani and M. Mirshafiei, *Colloid Nanosci. J.*, 2024, **1**, 203–207.
- 122 C.-y. Hui, B.-c. Ma, S.-y. Hu and C. Wu, *Environ. Pollut.*, 2023, 123016.
- 123 P. Deshpande, S. Wankar, R. Gumathannavar, S. Kulkarni, Y. Jadhav, Y. Patil, J. Rajwade and A. Kulkarni, *Nanocomposites*, 2024, **10**, 227–240.
- 124 S. Jiang, Z. Yan, Y. Deng, W. Deng, H. Xiao and W. Wu, *Int. J. Biol. Macromol.*, 2024, **262**, 129854.
- 125 E. J. Jang, B. Padhan, M. Patel, J. K. Pandey, B. Xu and R. Patel, *Food Control*, 2023, **153**, 109902.
- 126 Q. Feng, C. Wang, X. Miao and M. Wu, *Talanta*, 2024, **267**, 125224.
- 127 W. Hussain, X. Yang, H. Wang, M. Zhang, J. Zeng, M. W. Ullah, M. F. Awad, J. Hussain and S. Wang, *Int. J. Biol. Macromol.*, 2025, 146020.
- 128 S. Ghasemi, M. R. Bari, S. Pirsa and S. Amiri, *Carbohydr. Polym.*, 2020, **232**, 115801.
- 129 U. Farooq, M. W. Ullah, Q. Yang, A. Aziz, J. Xu, L. Zhou and S. Wang, *Biosens. Bioelectron.*, 2020, **157**, 112163.
- 130 A. Parnsubsakul, U. Ngoensawat, T. Wutikhun, T. Sukmanee, C. Sapcharoenkun, P. Pienpinijtham and S. Ekgasit, *Carbohydr. Polym.*, 2020, **235**, 115956.



- 131 L. Xiao, S. Feng, M. Z. Hua and X. Lu, *Talanta*, 2023, **254**, 124128.
- 132 A. El Sikaily, D. G. Ghoniem, O. Ramadan, E. M. El-Nahrery, A. Shahat and R. Y. Hassan, *Biochem. Eng. J.*, 2025, **216**, 109660.
- 133 E. Sheikhzadeh, S. Naji-Tabasi, A. Verdian and S. Kolahi-Ahari, *J. Iran. Chem. Soc.*, 2022, **19**, 283–290.
- 134 F. Bao, Z. Liang, J. Deng, Q. Lin, W. Li, Q. Peng and Y. Fang, *Crit. Rev. Food Sci. Nutr.*, 2024, **64**, 3920–3931.
- 135 K. Ludwicka, M. Kaczmarek and A. Białkowska, *Polymers*, 2020, **12**, 2209.
- 136 M. R. d. Santos, I. J. B. Durval, A. D. L. M. d. Medeiros, C. J. G. d. Silva Júnior, A. Converti, A. F. d. S. Costa and L. A. Sarubbo, *Foods*, 2024, **13**(20), 3327.
- 137 R. M. Abdelkader, D. A. Hamed and O. M. Gomaa, *World J. Microbiol. Biotechnol.*, 2024, **40**, 258.
- 138 S. Sadbangkean, S. Deangkamphon and P. Jaturapiree, *AIP Conf. Proc.*, 2023, **2669**(1), 040001.
- 139 B. Kuswandi, N. P. Asih, D. K. Pratoko, N. Kristiningrum and M. Moradi, *Packag. Technol. Sci.*, 2020, **33**, 321–332.
- 140 S. Mahović Poljaček, T. Tomašević, M. Stržić Jakovljević, S. Jamnicki Hanzer, I. Murković Steinberg, I. Žuvić, M. Leskovic, G. Lavrić, U. Kavčić and I. Karlovits, *Polymers*, 2024, **16**, 2259.
- 141 S. Yang, Q. Ding, Y. Li and W. Han, *Int. J. Biol. Macromol.*, 2024, **259**, 129203.
- 142 C. Hua, S. Gao, J. Wang, Y. Wang, J. Liu, F. Chen and X. Song, *Cellulose*, 2025, 1–15.
- 143 P. Lv, Y. Yao, D. Li, H. Zhou, M. A. Naeem, Q. Feng, J. Huang, Y. Cai and Q. Wei, *Carbohydr. Polym.*, 2017, **172**, 93–101.
- 144 D. Li, K. Ao, Q. Wang, P. Lv and Q. Wei, *Molecules*, 2016, **21**, 618.
- 145 G. Li, K. Sun, D. Li, P. Lv, Q. Wang, F. Huang and Q. Wei, *Colloids Surf., A*, 2016, **509**, 408–414.
- 146 E. Núñez-Carmona, A. Bertuna, M. Abbatangelo, V. Sberveglieri, E. Comini and G. Sberveglieri, *Mater. Lett.*, 2019, **237**, 69–71.
- 147 X. Li, D. Li, Y. Zhang, P. Lv, Q. Feng and Q. Wei, *Nano Energy*, 2020, **68**, 104308.
- 148 C. Zhao, G. Wang, M. Sun, Z. Cai, Z. Yin and Y. Cai, *Fibers Polym.*, 2021, **22**, 1208–1217.
- 149 A. R. Rebelo, C. Liu, K.-H. Schäfer, M. Saumer, G. Yang and Y. Liu, *Langmuir*, 2019, **35**, 10354–10366.
- 150 Z. Chen, Y. Hu, H. Zhuo, L. Liu, S. Jing, L. Zhong, X. Peng and R.-c. Sun, *Chem. Mater.*, 2019, **31**, 3301–3312.
- 151 T. Naghdi, H. Golmohammadi, M. Vosough, M. Atashi, I. Saeedi and M. T. Maghsoudi, *Anal. Chim. Acta*, 2019, **1070**, 104–111.
- 152 N. Cennamo, C. Trigona, S. Graziani, L. Zeni, F. Arcadio, G. Di Pasquale and A. Pollicino, *Sensors*, 2019, **19**, 4894.
- 153 H. Hosseini, M. Kokabi and S. M. Mousavi, *Carbohydr. Polym.*, 2018, **201**, 228–235.
- 154 S. Palanisamy, S. K. Ramaraj, S.-M. Chen, T. C. Yang, P. Yi-Fan, T.-W. Chen, V. Velusamy and S. Selvam, *Sci. Rep.*, 2017, **7**, 41214.
- 155 X. Ma, Y. Lou, X.-B. Chen, Z. Shi and Y. Xu, *Chem. Eng. J.*, 2019, **356**, 227–235.
- 156 G. Di Pasquale, S. Graziani, A. Licciulli, R. Nisi, A. Pollicino and C. Trigona, Geometrical Analysis of a Bacterial Cellulose-Based Sensing Element, *2019 II Workshop on Metrology for Industry 4.0 and IoT (MetroInd4.0&IoT)*, Naples, Italy, 2019, pp. 225–228.
- 157 S. Quraishi, S. Plappert, B. Ungerer, P. Taupe, W. Gindl-Altmutter and F. Liebner, *Appl. Sci.*, 2018, **9**, 107.
- 158 D. Qin, X. Hu, Y. Dong, X. Mamat, Y. Li, T. Wågberg and G. Hu, *J. Electrochem. Soc.*, 2018, **165**, B328.
- 159 V. V. Revin, E. V. Liyaskina, M. V. Parchaykina, T. P. Kuzmenko, I. V. Kurgaeva, V. D. Revin and M. W. Ullah, *Polymers*, 2022, **14**, 4670.
- 160 A. Rahman, S. Kang, W. Wang, Q. Huang, I. Kim and P. J. Vikesland, *ACS Appl. Nano Mater.*, 2022, **5**, 259–268.
- 161 Y.-T. She, C. K. Lin, G.-C. Zeng and Y.-L. Wang, Effective Training of AI Model with Diverse Data Augmentation Techniques for Biofet Sensors, in *Electrochemical Society Meeting Abstracts*, The Electrochemical Society, Inc., 2025, vol. 247(37), p. 1750.
- 162 Y. Zhao, X. Wang, T. Sun, P. Shan, Z. Zhan, Z. Zhao, Y. Jiang, M. Qu, Q. Lv, Y. Wang, P. Liu and S. Chen, *Biomeicrofluidics*, 2023, **17**(4), 041301.
- 163 D. K. X. Teo, T. Maul and M. T. T. Tan, Synthetic Electrochemical Biosensor Data with Conditional Variational Autoencoders for Enhanced Predictive Modeling, in *2024 IEEE SENSORS*, 2024, IEEE, pp. 1–4.
- 164 R. Bhaskar, M. Ola, S. Shinde, A. Pawar, V. Madwe, R. Tikhe and S. Khade, *J. Drug Deliv. Therapeut.*, 2025, **15**(8), 315.
- 165 J. Zhang, P. Srivatsa, F. H. Ahmadzai, Y. Liu, X. Song, A. Karpatne, Z. J. Kong and B. N. Johnson, *Biosens. Bioelectron.*, 2024, **246**, 115829.
- 166 Y. Zhao, X. Wang, T. Sun, P. Shan, Z. Zhan, Z. Zhao, Y. Jiang, M. Qu, Q. Lv, Y. Wang, P. Liu and S. Chen, *Biomeicrofluidics*, 2023, **17**, 041301.
- 167 C. D. Flynn and D. Chang, *Diagnostics*, 2024, **14**, 1100.
- 168 M. Astatke and C. Weng, Advancements in Machine Learning for Enhancing Sensitivity and Precision in Biological Sensing: A Comprehensive Review of Algorithms, Applications, and Challenges, in *Electrochemical Society Meeting Abstracts*, The Electrochemical Society, Inc., 2025, vol. 247(59), p. 2799, DOI: [10.1149/MA2025-01592799mtgabs](https://doi.org/10.1149/MA2025-01592799mtgabs).
- 169 K. Murugan, K. Gopalakrishnan, K. Sakthivel, S. Subramanian, I.-C. Li, Y.-Y. Lee, T.-W. Chiu and G.-P. Chang-Chien, *J. Electrochem. Soc.*, 2024, **171**, 097503.
- 170 D. L. Mancera-Zapata, C. Rodriguez-Nava, F. Arce and E. Morales-Narvaez, *Anal. Chem.*, 2024, **96**, 13756–13761.
- 171 V. Chirchi, E. Chirchi, E. C. Khushi, S. M. Bairavi and K. S. Indu, Optical Sensor for Water Bacteria Detection using Machine Learning, *2024 11th International Conference on Computing for Sustainable Global Development (INDIACom)*, New Delhi, India, 2024, pp. 603–608, DOI: [10.23919/INDIACom61295.2024.10498622](https://doi.org/10.23919/INDIACom61295.2024.10498622).
- 172 Y.-T. She, C. K. Lin, G.-C. Zeng and Y.-L. Wang, *ECS Meeting Abstracts*, 2025, vol. MA2025-01, p. 1750.



- 173 H. Li, H. Xu, Y. Li and X. Li, *TrAC, Trends Anal. Chem.*, 2024, **174**, 117700.
- 174 K. Icoz, in *Intersecting AI and Medicine for Improved Care and Administrative Efficiency*, IGI Global Scientific Publishing, 2026, pp. 163–216.
- 175 X. Wan, N. Li, J. Qiu, Q. Wang, Y. Feng and R. Xiong, *Biomacromolecules*, 2025, **26**, 5514–5546.
- 176 M. Saadi, Y. Cui, S. P. Bhakta, S. Hassan, V. Harikrishnan, I. R. Siqueira, M. Pasquali, M. Bennett, P. M. Ajayan and M. M. Rahman, *Nat. Commun.*, 2025, **16**, 5825.
- 177 A. Pandey, M. K. Singh and A. Singh, *J. Bioact. Compat. Polym.*, 2025, **40**, 94–116.
- 178 D. Absharina, F. J. N. Putra, C. Ogino, S. Kocsubé, C. Veres and C. Vágvolgyi, *Appl. Microbiol.*, 2025, **5**, 92.
- 179 S. Fei, M. Fu, J. Kang, J. Luo, Y. Wang, J. Jia, S. Liu and C. Li, *Curr. Res. Food Sci.*, 2024, **8**, 100761.
- 180 M. Ul-Islam, S. Yasir, L. Mombasawala, S. Manan and M. Wajid Ullah, *Curr. Nanosci.*, 2021, **17**, 393–405.
- 181 M. Weng, Y. Qiu, J. Zhou, H. Feng, N. Yi, Y. Zuo, J. Chen, P. Zhou, M. You and Q. Guo, *Chem. Eng. J.*, 2025, 167607.
- 182 Y. Ding, C. Hu, Y. Zhou, C. Wang, S. Zhang, J. Li, X. Lin and J. Xu, *ACS Appl. Nano Mater.*, 2025, **8**(27), 13806–13816.
- 183 P. P. Acharyya, M. Sarma and A. Kashyap, *Cellulose*, 2024, **31**, 7163–7187.
- 184 H. Zhao, L. Zhang, S. Zheng, S. Chai, J. Wei, L. Zhong, Y. He and J. Xue, *Carbohydr. Polym.*, 2022, **281**, 119017.
- 185 Q. Zhou, Q. Zhang, P. Wang, C. Deng, Q. Wang and X. Fan, *Fibers Polym.*, 2017, **18**, 1478–1485.
- 186 A. N. Shishparenok, V. V. Furman, N. V. Dobryakova and D. D. Zhdanov, *Polymers*, 2024, **16**, 2468.
- 187 S. Nadzirah, S. C. Gopinath, M. Ammar, C. F. Dee, U. Hashim, A. R. Md Zain and B. Yeop Majlis, *Crit. Rev. Anal. Chem.*, 2025, 1–23.
- 188 O. Mauger, S. Westphal, S. Klöpzig, A. Krüger-Genge, W. Müller, J. Storsberg and J. Bohrisch, *Plasma*, 2020, **3**, 196–203.
- 189 P. Tang, Y. Si, X. Song and G. Sun, *Cellulose*, 2024, **31**, 381–393.
- 190 Y. Wang, Q. Zhang, C. Ge, B. An and C. Zhong, *Acc. Mater. Res.*, 2024, **5**, 797–808.
- 191 S. Liu, M. Yang and W. Xu, *Chem Bio Eng.*, 2024, **1**, 876–886.
- 192 A. Ghosh, J. T. Orasugh, S. S. Ray and D. Chattopadhyay, *ACS Omega*, 2023, **8**, 28002–28025.
- 193 S. K. Parupelli and S. Desai, *Bioengineering*, 2023, **11**(1), 32.
- 194 A. S. Kulkarni, S. Khandelwal, Y. Thakre, J. Rangole, M. B. Kulkarni and M. Bhaiyya, *Biosensors*, 2025, **15**, 340.
- 195 J. Nyenhuis, C. Heuer and J. Bahnemann, *Chem.-Asian J.*, 2024, **19**, e202400717.
- 196 M. R. Binelli, P. A. Rühs, G. Pisaturo, S. Leu, E. Trachsel and A. R. Studart, *Biomater. Adv.*, 2022, **141**, 213095.
- 197 S. Maji, M. Kwak, R. Kumar and H. Lee, *Biosensors*, 2025, **15**(9), 619.
- 198 A. Sobhan, A. Hossain, L. Wei, K. Muthukumarappan and M. Ahmed, *Foods*, 2025, **14**, 1403.
- 199 T. Akkaş, M. Reshadsedghi, M. Şen, V. Kılıç and N. Horzum, *Adv. Mater.*, 2025, 2504796.

